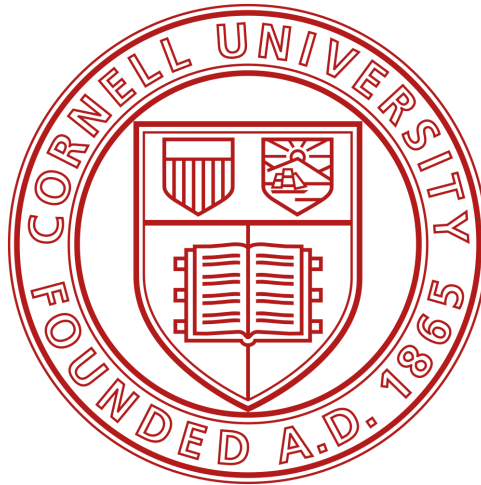


Effect of Fibrotic Layer Formation on Oxygen Delivery to Pancreatic Cells in a Cell Encapsulation Device


GABRIELLA BICA, IRENE CHAN, JEREMY WANG and LILY WOOLF



BEE 4530, Department of Biological and Environmental Engineering
Cornell University
Ithaca, NY

© Gabriella Bica, Irene Chan, Jeremy Wang, Lily Woolf, May 2020
gb447@cornell.edu, ic325@cornell.edu, jw2363@cornell.edu, lw543@cornell.edu

Contents

1. Executive Summary.....	3
2. Introduction	
2.1 Background and Literature Review.....	4
2.2 Problem Statement.....	5
2.3 Design Objective.....	6
3. Schematics	
3.1  device.....	7
3.2 1D Transfer Model.....	8
3.3 3D Transfer Model.....	9
4. Methods	
4.1 Assumptions.....	13
4.2 Governing Equations 1D, 3D.....	13
4.3 Boundary Conditions.....	14
5. Results and Discussion	
5.1 1D Model Results.....	16
5.2 3D Model Results.....	19
5.3 Sensitivity Analysis.....	28
5.4 1D Mesh Convergence.....	29
5.5 3D Mesh Convergence.....	30
5.6 Validation.....	32
6. Conclusion.....	34
7. Appendix A: Input Parameters.....	35
8. Appendix B: CPU and Memory Usage.....	37
9. Appendix C: Mathematical Methods.....	37
10. References.....	39

1. Executive Summary

Fibrosis is an immune response that handicaps the effectiveness of biomedical devices for individuals with type 1 diabetes. As an implant becomes encapsulated with connective tissue, forming a fibrotic layer, cells within a device may be unable to survive, leading to reduced performance. Recent studies have focused on fibrosis and its impact on insulin producing cells, but little research has explored the role fibrosis plays with regards to oxygen transfer.

Oxygen transfer into a pancreatic cell encapsulation device was explored in this study. Specifically, this device contains [REDACTED] surrounded by an alginate hydrogel with cells. When implanted, a fibrotic layer forms around the device; in this study, various thicknesses, compositions, and percent coverages of this layer were analyzed to observe their impact on survivability of cells due to limited oxygen availability.

In this study, oxygen transfer was explored within a [REDACTED] biomedical device with varying fibrotic layer thicknesses and percentages in order to observe the survival rate of insulin-producing cells within a hydrogel layer. The device used in this study contains an internal alginate hydrogel layer surrounded by a layer of fibrosis. The models were all built using COMSOL Multiphysics® Modeling Software and make use of oxygen diffusion from an external boundary condition and oxygen consumption based on Michaelis-Menten Kinetics. Under the 1D model, device oxygen levels were studied under varying severity of the fibrotic response and in several oxygen environments. Parameters including fibrotic layer thickness, seeding density within the hydrogel layer, and boundary oxygen concentration under full fibrotic layer coverage were varied. Results indicated that a higher seeding density results in lower concentration gradients, as more cells are present in the hydrogel and consuming more oxygen. Similarly, a thicker fibrotic layer results in less oxygen entering the hydrogel layer.

Under the 3D model, the effects of various percentages and thickness of the fibrotic layer were studied, with coverages varying in intervals of 25%. In the scenario of 100% fibrotic layer coverage at 200µm thickness, the model indicates most cells in the hydrogel become necrotic due to the limited oxygen and high oxygen consumption from the fibrotic layer. Under a more idealized situation with 25% coverage of fibrotic tissue at 10µm thickness, oxygen concentration is still depleted but less egregiously, with little risk of necrosis. The sensitivity analysis indicates how the model is more sensitive to subtle changes in seeding density and surface oxygen concentration, as opposed to other parameters. Data obtained in the study was validated via comparisons with oxygen concentrations within the fibrotic layer from another existing 1D analytical model. Similarly, oxygen concentration in the hydrogel region of the 3D model was compared to data obtained from another study measuring oxygen concentration within a device encapsulated by fibrosis. Overall, the results emphasize the importance in eliminating any possible fibrotic encapsulation around a biomedical device.

Keywords: Alginate hydrogel, Diabetes, Fibrosis, Encapsulated Cells, COMSOL Multiphysics

2. Introduction

2.1 Background and Literature Review

Type 1 diabetes mellitus is an autoimmune disease associated with the destruction of insulin producing β -cells. Type 1 diabetes accounts for 5-10% of all cases of diabetes, with this figure rising by 3% each year [1]. Those suffering from type 1 diabetes produce little to no insulin, leading to an inability to regulate blood glucose levels. The disorder has a strong genetic component, inherited mainly through the HLA complex, but the factors that trigger onset of clinical disease remain largely unknown [2]. At present, no cure is available, and conventional treatment for type 1 diabetes is complex and inefficient. Patients often require two or more daily injections of insulin or treatment with an external insulin pump, constant self-monitoring through measurement of glucose levels in order to avoid hypoglycemia, and a strictly monitored diet plan [3]. This monitoring and treatment plan is difficult for those dealing with the disease; as a result, research in recent years has turned to the possibility of implantable devices as effective treatments causing fewer lifestyle changes and less intensive monitoring.

Although these implantable medical devices are considered biocompatible by the Food and Drug Administration, the inflammatory response composed of macrophages and foreign body giant cells following implantation of a medical device is a leading cause of their failure [4]. This foreign body response leads to fibrosis, or encapsulation of the device by excess connective tissue made of immune cells that form a layer of varying thickness around the device. This is predicted to result in a reduction or cessation of device performance, as well as increasing risk of microbial infection [5]. Although there is much room for improvement, it is extremely important to continue research on these implantable devices, as they will allow type 1 diabetes patients to live a more manageable lifestyle.

Currently, one area of research is focused on creating an implantable device to mimic the function of a healthy human pancreas by encapsulating pancreatic islet cells in an alginate hydrogel membrane [6]. Due to biocompatibility of mammalian cells and the scarcity of medically available healthy human pancreatic β -cells, studies are being done on the possibility of using modified porcine islet cells or induced pluripotent stem cells modified from other cells taken from the patient [7]. The encapsulation of these cells in an alginate hydrogel layer prevents immune recognition in the body and allows the encapsulated cells to sense glucose through diffusive transport of intermediate macromolecules. However, the formation of a fibrotic layer around these hydrogels limits oxygen transfer to encapsulated cells, inhibiting cell growth, survival, and insulin production. In addition, the transport of larger molecules such as glucose and insulin into and out of the device may be slowed to ineffective levels, preventing encapsulated cells from accurately sensing glucose level and hindering insulin transport into the bloodstream [7]. This case study develops a model with the goal of understanding the effect of

the fibrotic layer on the survival and efficacy of insulin producing cells encapsulated in a hydrogel.

Creating an accurate model to understand the influence of the fibrotic layer is worth pursuing because modeling can aid in quantitatively characterizing the transport of oxygen, glucose, and insulin through known governing mass transport equations and Michaelis-Menten kinetics. The model considers many variables including fibrotic layer thickness, seeding density of the hydrogel, thickness of the hydrogel, and blood oxygen concentration. By creating a model that incorporates all of these components, the ideal properties to maximize utility of such an implantable device can be studied, while reducing expensive, labor-intensive, and time-consuming in vivo experimentation. In order to accurately model this complex system, computational programs must be used. Development of the model used COMSOL Multiphysics®, which resolves mass transport equations through a given geometry model using finite element analysis. The initial problem formulation for oxygen transfer in this context studied how oxygen tensions in the environment of biomedical devices may prohibit performance [8]. A recent study in this area [9] investigating the influence of oxygen in the secretory capacity of insulin in pancreatic islets led to the conclusion that oxygen consumption rate is affected by islet size. However, this study did not incorporate details of the influence that fibrotic layer formation may have on the device. By determining how fibrosis may affect oxygen transport, the goal is to gain a better understanding of the effects of fibrosis on encapsulated cells. Specifically, as there are poor means of quantifying this effect in vitro/vivo, modeling should allow for the efficient study of this effect with a known set of parameters. This will contribute to the production of a working device for type 1 diabetes treatment and optimization of the design of other medical devices.

This model was developed in collaboration with the Ma Laboratory at Cornell University and Ohio State University to study a [redacted] cell encapsulation [redacted] device with cylindrical geometry and multiple layers. The device is made of two concentric cylinders: a [redacted] scaffold in the center, surrounded by a layer of alginate hydrogel containing islet cells that can be approximated as being uniformly distributed. [redacted] response is intended to reduce fibrosis; the obtained data should help determine the maximum fibrotic layer thickness permissible for maintaining survival and function of the encapsulated cells in the device. In this study, the device was modeled as three concentric cylinders, with the outermost layer composed of the fibrotic cells. This model considers transport in only the hydrogel and fibrotic layers.

2.2 Problem Statement

The purpose of this study is to model the diffusion of oxygen into the [redacted] hydrogel cell encapsulation device in order to determine the effect of fibrotic layer formation on the

effectiveness as a treatment for type I diabetes. The [redacted] device is still under production by the Ma Laboratory at Cornell University, but the hope is that it will be used as a replacement for repeated insulin injections and intensive blood sugar monitoring in type 1 diabetes patients. Oxygen must diffuse into the device to reach the pancreatic cells so that those cells can survive and produce insulin as intended. In order to accurately model this process, the thickness and composition of the fibrotic layer surrounding the implanted device must be considered as it adds a mass transfer resistance, limiting oxygen transport to the encapsulated cells. The process being modeled is the diffusion and simultaneous consumption of oxygen by cells in the fibrotic layer and the hydrogel. The goal is to determine how to better design a device so that the majority of cells can survive. This physical modeling of diffusion into an implanted device will hopefully find future applications for other implantable devices and allow for better design to optimize diffusion of all components.

Given the complex nature of the problem, it is difficult to characterize the effects of various fibrotic layer thicknesses and compositions. This device has not been put into clinical trials yet and therefore computational modeling provides one of the quickest and most effective ways to determine the effects of various fibrous responses to device implantation. This information is important in determining whether reducing fibrosis has a meaningful effect on cell survival, and therefore whether or not it is worth trying to minimize it. Further, this paper will focus on identifying acceptable and unacceptable levels of fibrosis, since the formation of a fibrotic layer is likely not an entirely avoidable phenomenon.

2.3 Design Objective

This study aims to contribute to existing research on islet encapsulation in the following ways:

1. Providing an increased understanding of oxygen availability to pancreatic beta cells at different encapsulation densities within an alginate hydrogel layer.
2. Exploring the impact of varying thicknesses and percent coverages for the fibrotic layer on oxygen transport.
3. Determining the relative impact of various input parameters on oxygen concentration through a sensitivity analysis.

3. Schematics

3.1 Device

The Device is intended to be used as a treatment for type 1 diabetes by encapsulating pancreatic cells in the device and . The function of cellular encapsulation is to create an environment to isolate implanted foreign cells and prevent them from being targeted by the body's immune response. This allows the pancreatic cells of another human or species to be implanted in a patient with type 1 diabetes without the body recognizing that the cells are foreign, allowing them to function and produce insulin as needed [7]. Cell clusters for implantation are either grown from insulin-producing stem cells, or isolated from animals (including human donors), and then encapsulated and implanted [7]. These can be seen in the illustration of the Device in Figure 1, which represents the cell clusters, or islets, as blue circles. The scaffold can be seen running through the center of the device, and is the key feature giving the Device its name.

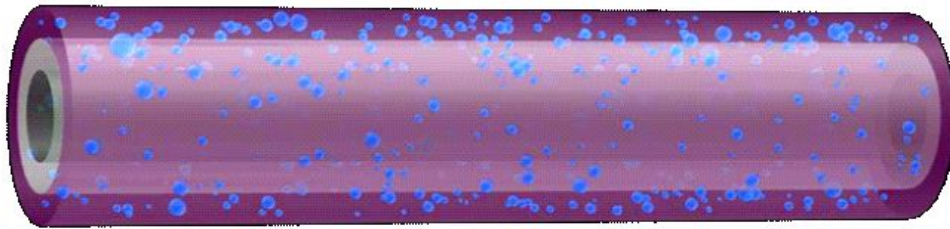


Fig. 1 *Illustration of the Device.* The center of the device contains a scaffold, shown in grey, surrounded by the alginate hydrogel in purple. The blue clusters represent pancreatic islets. Included with permission from Alexander Ernst, Ma Lab, Cornell University.

A visual of oxygen molecules travelling into the model can be seen in Figure 2, which displays the portions of the Device that were modeled and contain cells: the fibrotic layer and the hydrogel.

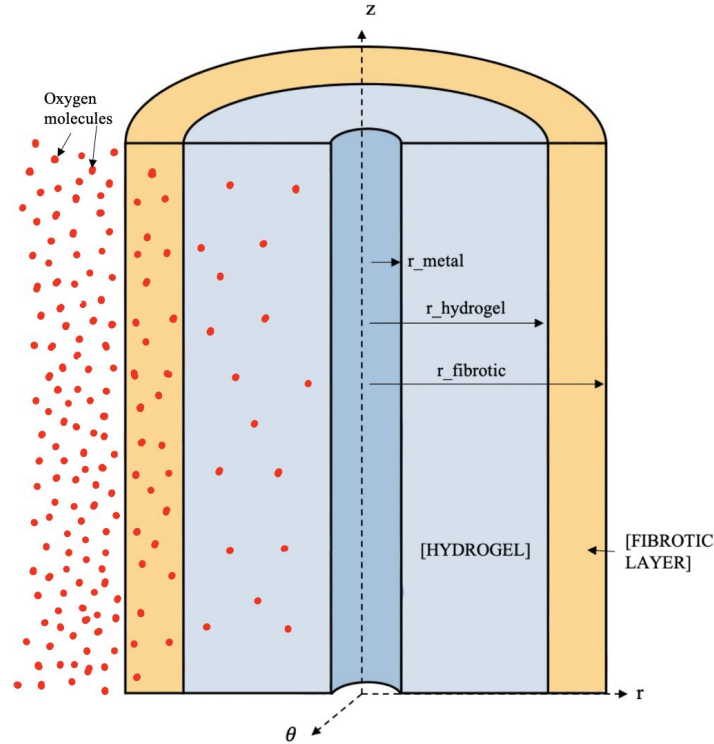
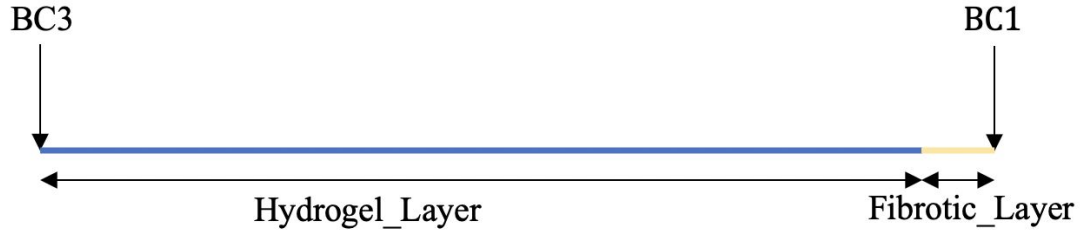


Fig. 2 Visual of the [redacted] device model. Oxygen molecules shown in red travel through the device via diffusion and are consumed by fibrotic and encapsulated cells. The yellow region represents the fibrotic layer and the light blue region is the hydrogel. See Figure 4 for further explanation of device dimensions.

3.2 1D Transfer Model

The system was first modeled in 1D in order to show oxygen transport into the device. The device has two layers: an inner [redacted] core and the alginate hydrogel with pancreatic cells uniformly dispersed. The model only contains the alginate hydrogel layer, and also includes an outer layer of fibrosis formed during the body's immune response. The model does not contain the [redacted] core, as oxygen transport into this scaffold is not pertinent to the study of encapsulated cells. This model assumes an even distribution of fibrosis on the outside of the [redacted] device; this translates to a constant fibrotic thickness length, which allows for the model to be sufficient in one dimension. As the model is only one dimensional, “inner” corresponds to the leftmost boundary, while “outer” corresponds to the rightmost boundary. A detailed schematic is shown in Figure 3, in which oxygen diffuses through the fibrotic layer into the hydrogel, where it can reach the pancreatic cells.



1D Model

$$\text{BC1: } c_{O_2}|_{r=r_{fibrotic}} = c_{surface}$$

$$\text{BC3: } \frac{\partial c_{O_2}}{\partial r}|_{r=r_{metal}} = 0$$

Fig. 3 1D schematic of the device. This shows two layers of the device: the alginate hydrogel with pancreatic islets, and the fibrotic layer. The hydrogel has a length of *Hydrogel_Layer*, and the fibrotic layer has a length of *Fibrotic_Layer*. There is a constant concentration boundary condition at the outside of the fibrotic layer ($r=r_{fibrotic}$). There is a zero flux boundary condition at the hydrogel-metal boundary ($r=r_{metal}$), as no oxygen diffuses into the metal core.

The 1D model from Figure 3 was used to model oxygen transport into the device when the fibrotic layer formed uniformly. This allowed the study of various parameters and their impact on the transport of oxygen, including diffusivity constants, oxygen consumption rates, and other characteristics of the two regions.

3.3 3D Transfer Model

Although a 1D model is sufficient to represent the physics of the diffusion of oxygen into the device given a constant fibrotic layer thickness, when modeling the possibility of 25%, 50%, and 75% fibrotic layer coverage, it was necessary to build a model in multiple dimensions. Oxygen transport is being modeled in two dimensions: radially and azimuthally. Although the model could have sufficiently been run in 2D, the model was designed in 3D to provide a more comprehensive visual of oxygen concentration variations across the device.

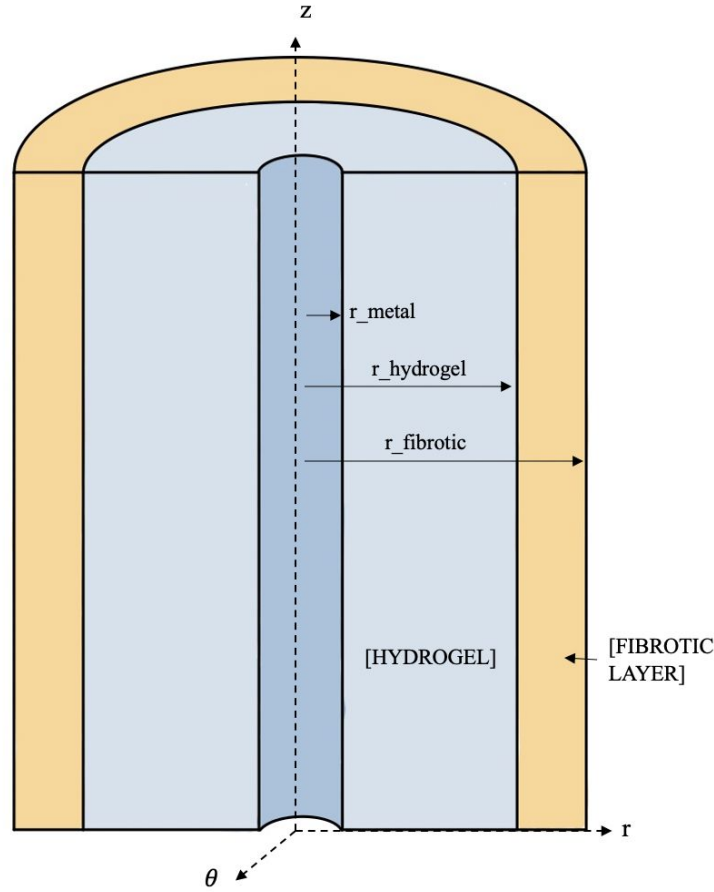
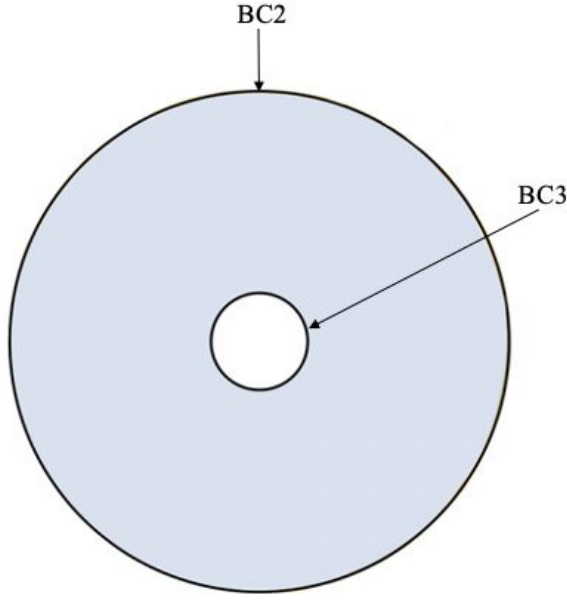


Fig. 4 Cross-section of the 3D model. The empty core represents the location of the scaffold with a radius of r_{metal} . The blue region is the hydrogel, which contains pancreatic cells distributed with a given seeding density. The radius of this region is $r_{hydrogel}$. The yellow region is the fibrotic layer surrounding the device, with a radius of $r_{fibrotic}$.

In addition to the 3D cross-sectional model shown in Figure 4, a 2D cross sectional schematic was created in order to concisely represent the domain over which the diffusion and reaction terms in this model occur. Boundary conditions (BCs) describing conditions on the boundary of the models are displayed to the right of schematics for Models A-E, seen in Figures 5-7 below.

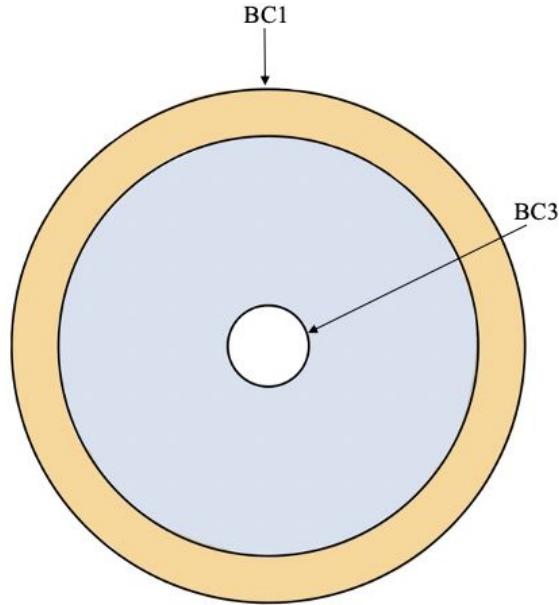


Model A

BC2: $c_{O_2} = c_{surface}$

BC3: $\frac{\partial c_{O_2}}{\partial r} \big|_{r=r_{metal}, z=0} = 0$

Fig. 5 Model A. A schematic of the device with no fibrosis. The white core is the scaffold with a radius of r_{metal} . The center is surrounded by a hydrogel layer (blue) with a radius of $r_{hydrogel}$. This model assumes that no fibrosis has occurred, so it lacks a fibrotic layer. The labeled boundary conditions are listed above, and explained in Section 4.3.



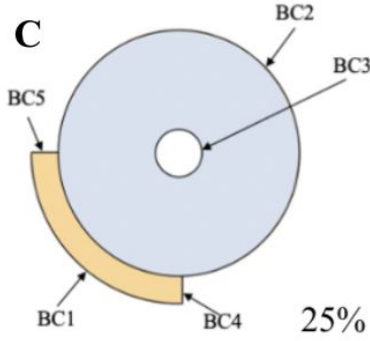
Model B

BC1: $c_{O_2} \big|_{r=r_{fibrotic}, z=0} = c_{surface}$

BC3: $\frac{\partial c_{O_2}}{\partial r} \big|_{r=r_{metal}, z=0} = 0$

Fig. 6 Model B. A schematic of the device fully encapsulated by fibrosis. The white core is the scaffold with a radius of r_{metal} . The center is surrounded by a hydrogel layer, shown in blue, with a radius of $r_{hydrogel}$. This model assumes complete fibrosis, so the hydrogel

layer is completely surrounded by an outer fibrotic layer in yellow with a radius of $r_{fibrotic}$. The labeled boundary conditions are listed above, and explained in Section 4.3.



Models C-E

BC1: $c_{O_2}|_{r=r_{fibrotic}, z} = c_{surface}$

BC2: $c_{O_2}|_{r=r_{hydrogel}, z} = c_{surface}$

BC3: $\frac{\partial c_{O_2}}{\partial r}|_{r=r_{metal}, z} = 0$

BC4: $c_{O_2} = c_{surface}$

BC5: $c_{O_2} = c_{surface}$

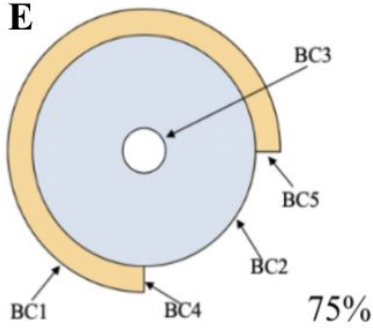
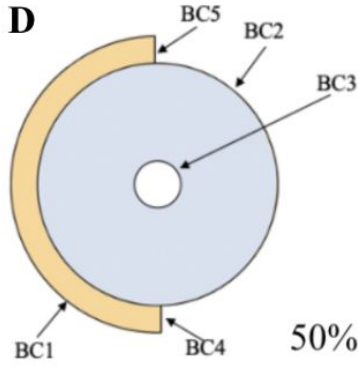



Fig. 7 Models C, D, and E. Schematics of the device with varying degrees of fibrosis. These models assume partial fibrosis, so the hydrogel layer is only partially surrounded by an outer fibrotic layer (in yellow). The labeled boundary conditions are listed above, and explained in Section 4.3.

4. Methods




4.1 Assumptions

Various assumptions were made when developing the model for oxygen diffusion into the hydrogel. In terms of geometry, axial symmetry of the cylindrical model at steady state was assumed. It was assumed that no oxygen diffused into the  core. The device was further simplified so the cells were evenly distributed in the hydrogel portion of the device with a seeding density of 2%, instead of in islet clusters. This allowed for a model that averaged the oxygen consumption across the entire volume of the device, eliminating variation due to different densities of cells in various regions.

The model has no time dependency because the device would remain in the body for long periods of time. This would result in constant concentrations of all chemical species, as the time when the device reaches a steady state occurs during the lengthy placements necessary for type 1 diabetes treatment. The rate of consumption of oxygen was modeled by Michaelis-Menten kinetics within both the fibrotic and hydrogel layers [8]. However, the oxygen consumption rate varied between the two layers due to differing cell densities and properties, resulting in different reaction terms. We ignored a modulating factor used to account for changing glucose concentrations as we are primarily interested in oxygen diffusion. Convective transport of oxygen was assumed to be negligible as there is no significant bulk flow of oxygen within the domain.

Constant diffusion coefficients were assumed within each layer of the domain, and the accepted literature value of the diffusion coefficient of water through tissue was adopted as the diffusion coefficient of oxygen transport through the fibrotic tissue layer. They are assumed to be very similar due to the high moisture content of alginate hydrogels [10]. The diffusivity for the fibrotic layer was assumed to be the same as native collagen scaffolds [11]. The partition coefficient between the hydrogel and fibrotic layer was neglected since it is close to one based on previous experimental measurements [12]. The partition coefficient between the fibrotic layer and the surrounding tissue was also neglected based on the same assumption.

4.2 Governing Equations 1D, 3D

The physics of the model implemented in this study involved the mass transfer of oxygen, as well as reactions occurring within both the hydrogel and fibrotic layer of the device, serving as a consumption term of oxygen. The steady-state model accounts for the travel of oxygen through the fibrotic and hydrogel layers of the device to the  core boundary via the implementation of constant concentration boundary conditions at the outermost surface of the fibrotic layer, and a zero flux boundary condition at the  core boundary. The  core was excluded from the oxygen transfer model because no oxygen is present in this domain, and there are no cells in this region requiring oxygen for survival. As a result, a single governing

equation has been implemented across the fibrotic layer and hydrogel domains separately, with varying parameters.

The reaction term in each of these layers was represented by R_{oxy} in Equation 1, which varied for the different regions. The different values of diffusivity and oxygen consumption rate were accounted for, and distinguish the alginate hydrogel and fibrotic tissue. The values for parameters used are found in Appendix A. Equation 1 shows only radial transport, represented in this model in the r direction and used in the 1D models. The addition of oxygen diffusion in the ϕ direction was included in the 3D models, as shown in Equation 2 and accounted for uneven fibrotic layer coverage.

1D Diffusion

$$0 = D \left[\frac{1}{r} \frac{\partial}{\partial r} \left(r \frac{\partial c_{O_2}}{\partial r} \right) \right] - R_{oxy} \quad (1)$$

3D Diffusion (uneven fibrosis)

$$0 = D \left[\frac{1}{r} \frac{\partial}{\partial r} \left(r \frac{\partial c_{O_2}}{\partial r} \right) + \frac{1}{r^2} \left(\frac{\partial^2 c_{O_2}}{\partial \phi^2} \right) + \frac{\partial^2 c_{O_2}}{\partial z^2} \right] - R_{oxy} \quad (2)$$

The reaction term for oxygen was calculated using Michaelis-Menten kinetics, which is normally used to model enzyme kinetics but also widely used in cellular respiration kinetics modeling. This is shown below in Equations 3 and 4. The percentage of cells, which relates to the consumption rate, is accounted for by multiplying the Michaelis-Menten reactions by a seeding density of cells within the hydrogel, ρ_{islets} , representing the volume fraction of the cells in the hydrogel. The model assumed uniform cell distribution instead of cell clusters, as would be in the device, for ease of modeling.

Michaelis-Menten: Hydrogel

$$R_{oxy} = \rho_{islets} R_{max,oxy,hydro} \frac{c_{O_2}}{c_{O_2} + c_{Hf,oxy}} \quad (3)$$

Michaelis Menten: Fibrotic Layer

$$R_{oxy} = R_{max,oxy,fib} \frac{c_{O_2}}{c_{O_2} + c_{Hf,oxy}} \quad (4)$$

4.3 Boundary Conditions

Boundary conditions 1-5, as implemented in the 1D and 3D models are summarized below. See Figures 3, 5-7 for schematics showing their locations.

Boundary Condition 1 (BC 1) in Equation 5 represents the constant oxygen concentration, $c_{surface}$, that is found at the surface of the fibrotic layer that forms on the outside of

the device. The constant oxygen concentration is the concentration in the tissue that surrounds the device.

$$c_{O_2}|_{r=r \text{ fibrotic}, z} = c_{\text{surface}} \quad (5)$$

Boundary Condition 2 (BC 2) in Equation 6 represents the constant oxygen concentration, c_{surface} , that is found at the surface of the hydrogel when there is no fibrotic layer formation, and the hydrogel is in direct contact with surrounding tissue.

$$c_{O_2}|_{r=r \text{ hydrogel}, z} = c_{\text{surface}} \quad (6)$$

Boundary Condition 3 (BC 3) in Equation 7 represents the zero flux condition at the interface between the hydrogel and the scaffold at the core of the model. It is assumed that no oxygen diffuses into the core.

$$\frac{\partial c_{O_2}}{\partial r}|_{r=r \text{ metal}, z} = 0 \quad (7)$$

Boundary Conditions 4 and 5 (BC 4, 5) in Equation 8 represent the constant oxygen concentration, c_{surface} , that is found on the edges of the fibrotic layer that come in contact with surrounding tissue when the fibrotic layer is not completely enclosing the device. This is applicable to Models C-E.

$$c_{O_2} = c_{\text{surface}} \quad (8)$$

Boundary Conditions 6 and 7 in Equations 9 and 10 represent the zero flux condition at the end caps of the model, as any flow was ignored.

$$\frac{\partial c_{O_2}}{\partial z}|_{z=0, r} = 0 \quad (9)$$

$$\frac{\partial c_{O_2}}{\partial z}|_{z=L, r} = 0 \quad (10)$$

5. Results and Discussion

In order to develop the finalized model for the figures obtained in this study, standardized values were chosen for the following parameters: fibrotic layer thickness, oxygen concentration at the fibrotic layer boundary, and pancreatic cell density within the hydrogel. These values were then maintained and assumed throughout the remainder of the study. Parametric sweeps were run for the aforementioned parameters to choose appropriate values and aid in the sensitivity analysis.

5.1 1D Model Results

As the main focus of this study was determining the effect of the fibrotic layer on oxygen transport within the device, choosing a logical fibrotic layer thickness was essential to the

overall design. Figure 8 below illustrates the effect of changing fibrotic layer thickness on oxygen concentration within the hydrogel and fibrotic layer of the device.

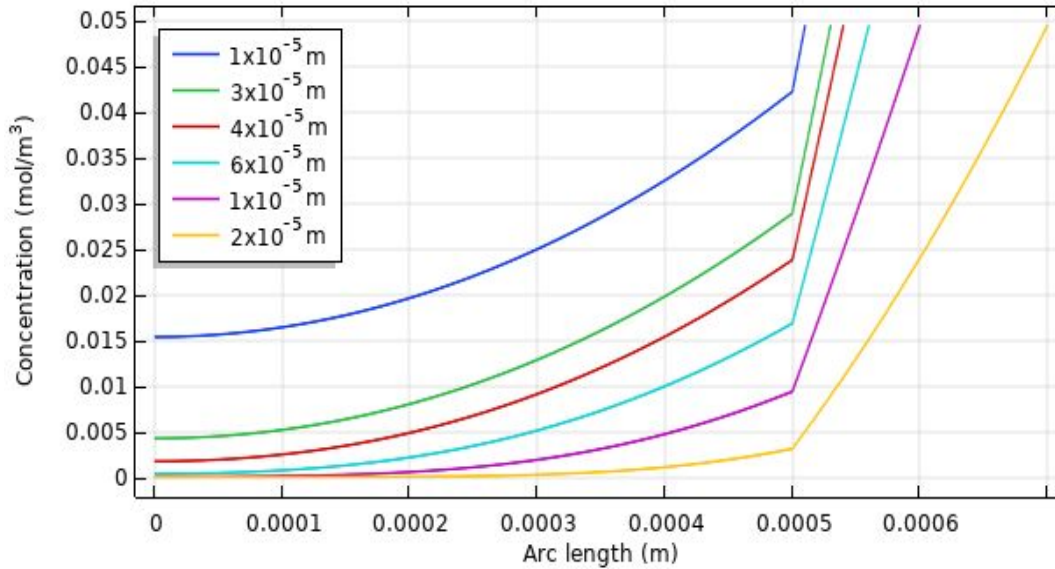


Fig. 8 Parametric sweep of seven different fibrotic layer thicknesses. A parametric sweep was done for seven fibrotic layer thicknesses ranging from 10 μ m to 200 μ m. An arc length of 0 μ m in this graph corresponds to the [redacted] core/hydrogel interface, and an arc length of 500 μ m corresponds to the hydrogel/fibrotic layer interface, as indicated on the x-axis.

The results shown in Figure 8 make physical sense, as a thicker fibrotic layer results in less oxygen entering the hydrogel at the hydrogel/fibrotic layer interface. The change of slope observed at 5 μ m is due to the differences in consumption of oxygen and diffusivity between the hydrogel and fibrotic layer portions of the device. When developing the 1D model for this study, a fibrotic layer of 40 μ m thickness was chosen.

Figure 9 uses the same process, this time generating an oxygen concentration profile under various oxygen concentrations at the outer boundary of the fibrotic layer. The parametrization was conducted with surface oxygen partial pressures of 24mmHg, 40mmHg, and 60mmHg, reflecting the range of oxygen partial pressures in human tissue [13].

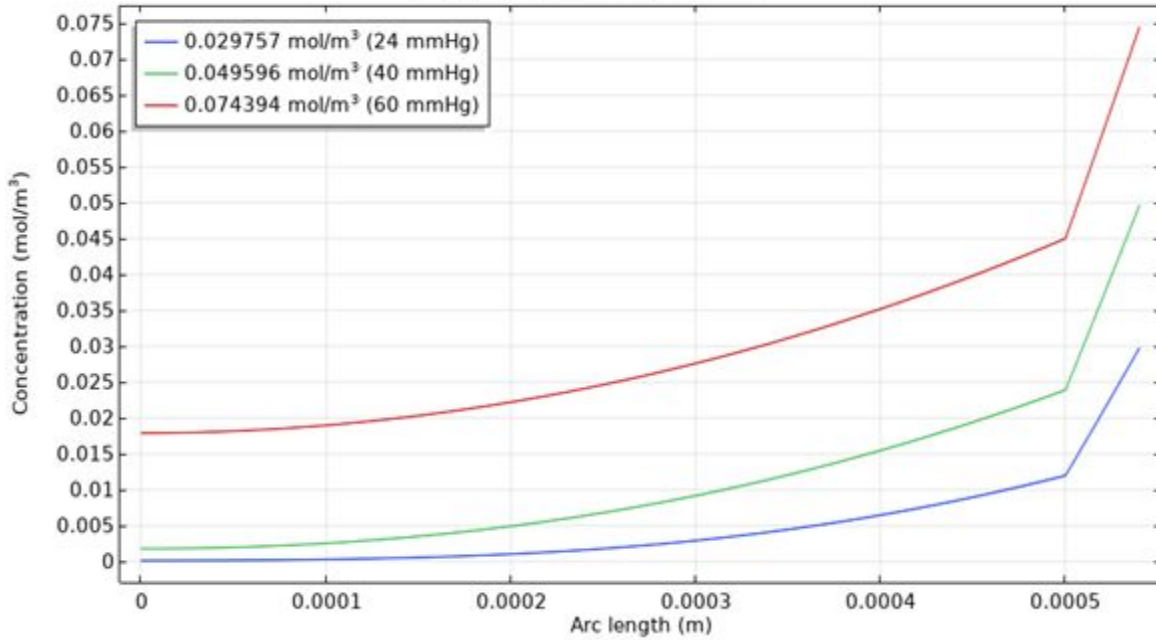


Fig. 9 Parametric sweep for oxygen concentration at the outside boundary of the fibrotic layer. A parametric sweep was done for varying oxygen concentrations at the hydrogel-fibrotic layer interface. An arc length of 0 μm in this graph corresponds to the [redacted] core-hydrogel boundary, and an arc length of 500 μm corresponds to the hydrogel-fibrotic layer boundary. The green center line shows the concentration profile of oxygen through the hydrogel if the oxygen concentration at the boundary is equivalent to 40 mmHg.

According to previous research, the critical concentration of oxygen necessary for cell survival is $1 \times 10^{-4} \text{ mol/m}^3$ [10]. The results obtained from the parametric sweep indicate that regions in the hydrogel never reach the critical concentration for all surface concentrations studied. However, at a surface concentration of 24 mmHg, cells near the [redacted] core experience oxygen concentrations very close to the critical value. Although these cells would not necessarily undergo necrosis, they would still have difficulty performing cellular functions such as producing insulin. A surface oxygen concentration of 0.049596 mol/m^3 , which is equivalent to a partial pressure of 40 mmHg, was chosen as the parameter for all further models as it represents a commonly accepted value for venous oxygen concentration [13]. The change in slope exhibited at arc length of 500 μm is also expected, as it reflects the changing material from alginate hydrogel to fibrotic layer tissue.

Another parametric sweep was conducted in order to study the effects of pancreatic cell seeding density within the hydrogel layer of the device. Seeding density in this model represents the percent of the hydrogel made up of islet cells by volume. Realistic seeding densities for this model based on the laboratory development of the [redacted] device range from 1% to 5%, as reflected by the varying parameters chosen in the parametrization shown in Figure 10.

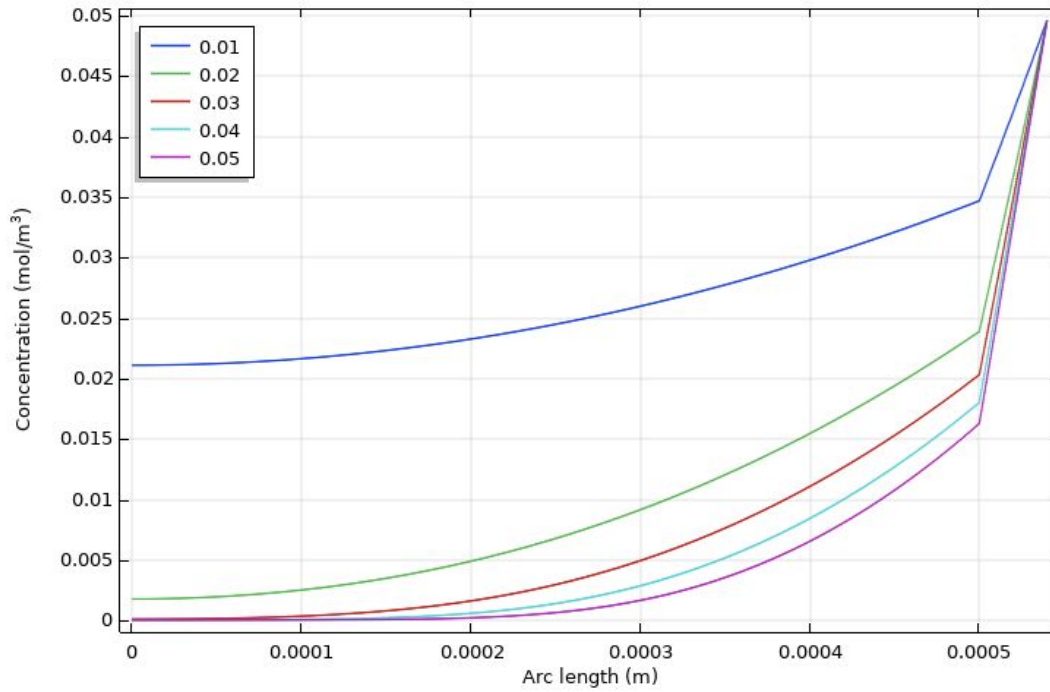


Fig. 10 *Parametric sweep of different hydrogel seeding densities.* A parametric sweep of seeding densities was done at 1% increments ranging from 1% to 5%, with the top blue line representing 1% and the bottom purple line representing 5% seeding densities. An arc length of 500 μ m again corresponds to the hydrogel-fibrotic layer boundary.

Results obtained from the parametric sweep in Figure 10 show that data representing higher seeding density causes a steeper drop in oxygen concentration. This makes physical sense, since greater seeding density means that there are more cells consuming oxygen within the hydrogel layer, which causes a steeper decrease in oxygen concentration in that region. The higher oxygen consumption in the hydrogel layer also lowers the oxygen concentration at the hydrogel/fibrotic layer interface, resulting in a steeper oxygen gradient in the fibrotic layer as shown in Figure 10. The curves obtained are consistent with what is expected from Michaelis-Menten kinetics, as the rate of oxygen consumption becomes limited in low oxygen environments [10].

One last parametric sweep was conducted by varying the degree of immune cell infiltration in the fibrotic layer. Fibrotic layers often contain oxygen-consuming immune cells such as macrophages [14]. It was important to study the effects that varying amounts of immune cells could have on oxygen consumption in the fibrotic layer, as increased immune cell infiltration could greatly decrease the amount of oxygen that enters the hydrogel. In the parametric sweep shown in Figure 11 below, immune cell infiltration was defined as the density of macrophages in the fibrotic layer and the parametric sweep was conducted with macrophage densities ranging from 1×10^6 to 50×10^6 cells/mL.

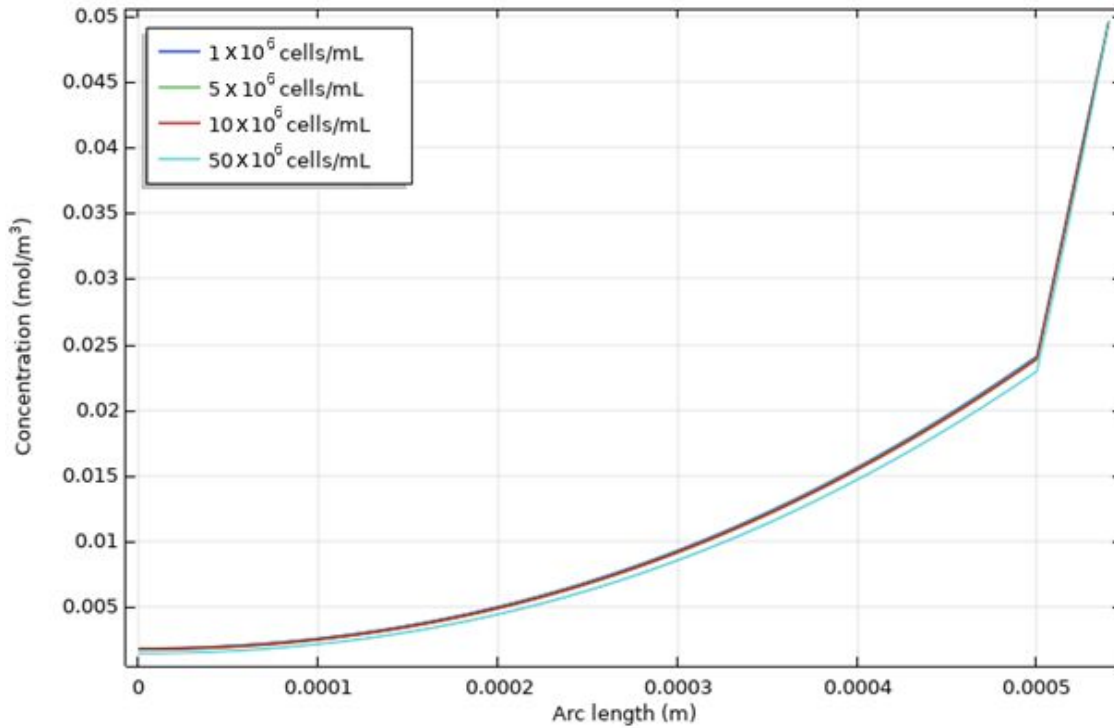


Fig. 11 *Parametric sweep of different degrees of immune cell infiltration within the fibrotic layer.* A parametric sweep was done for various macrophage densities in the fibrotic layer, ranging from 1×10^6 to 50×10^6 cells/mL. An arc length of $500 \mu\text{m}$ corresponds to the boundary between the hydrogel and fibrotic layer.

The results in Figure 11 indicate that varying macrophage density in the fibrotic layer has little effect on oxygen concentration in the hydrogel. The concentration profile shows little change after a 50-fold increase in macrophage density. One reason for this could be that the chosen fibrotic layer thickness of $40 \mu\text{m}$ is too thin to see the effects of increasing macrophage density. For thicker fibrotic layers, the difference in oxygen concentration entering the hydrogel would be more noticeable. This effect still expected to be negligible in comparison to the effect of an increased fibrotic layer thickness presenting a diffusive resistance.

5.2 3D Model Results

The same model was then implemented in 3D, with the purpose of analyzing the effect of various fibrotic layer formations on the device. Five models created with fibrosis covering different percentages of the device: 0%, 100%, 25%, 50% or 75%. These five models are referred to as models A, B, C, D, and E, respectively, and schematics of each are found in Figures 5-7 above.

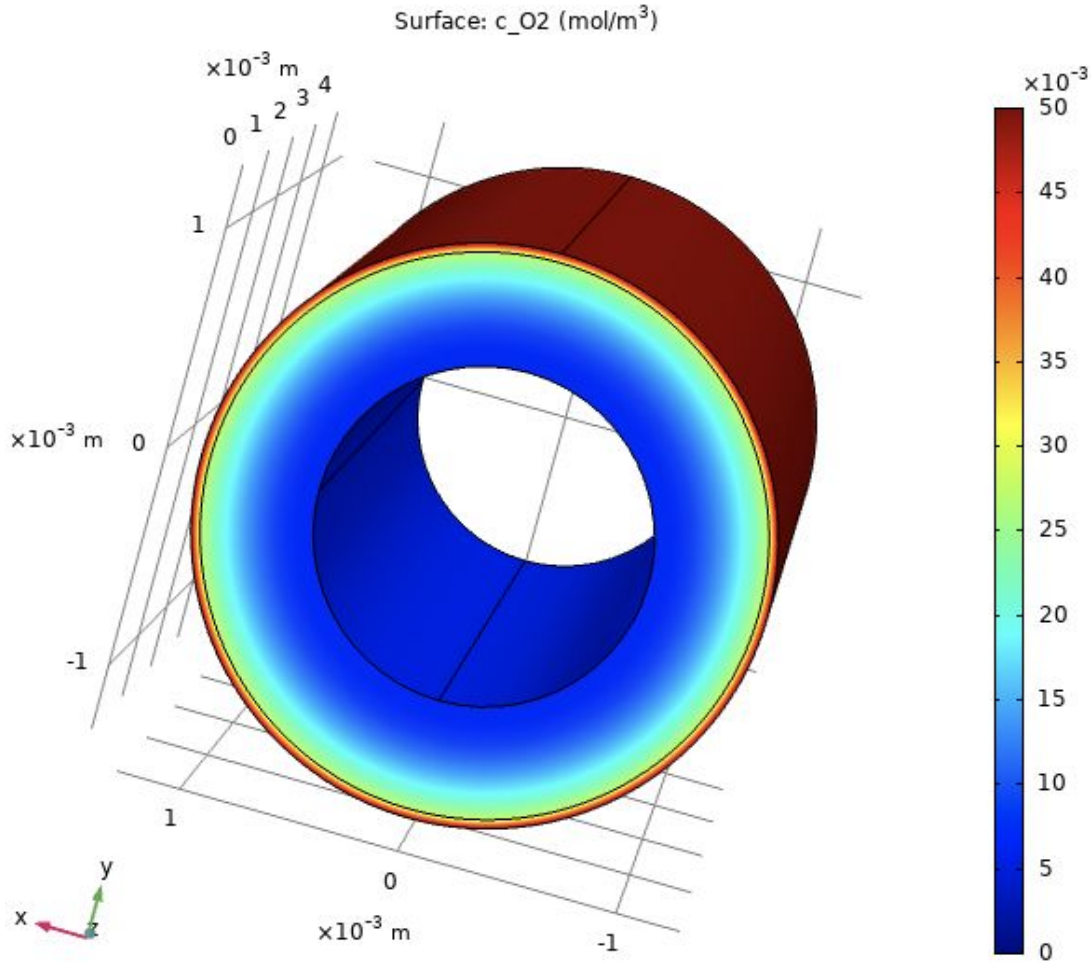


Fig. 12 3D model of fibrotic layer formation around device. Modeled with fibrotic layer thickness of $40\mu\text{m}$ (as was done for 1D models) and fibrosis entirely encapsulating the device. The fibrotic layer is a clear impediment to oxygen transport, as the red and orange regions of high oxygen concentration are all in the fibrotic layer, and the concentration of oxygen has decreased significantly within the fibrotic layer, as shown in the green/blue regions. The color scale of oxygen concentration values, in mol/m^3 , is shown on the right of the model.

The 3D model shows that many of the cells within the hydrogel are unable to obtain adequate oxygen levels for insulin production and survival. Although the critical oxygen value for cell survival is $1 \times 10^{-4} \text{mol/m}^3$ [10], studies in rat and canine islets have shown a 50% decrease rate in insulin production at 27mmHg, or 0.033477mol/m^3 , and a 98% decrease at 5mmHg, or 0.0061995mol/m^3 [15]. An oxygen concentration of 0.033477mol/m^3 , which indicates a 50% decrease in the rate of insulin production, is depicted by the yellow regions in the surface plot. In the region where light blue turns to dark blue, towards the center of the device, oxygen concentration is approximately 0.0061995mol/m^3 and insulin production is reduced by 98%. This means that the model as designed will result in cells unable to produce necessary amounts of

insulin in a large portion of the center of the hydrogel. When attempting to increase insulin production and reduce the likelihood of cell death, various parameters were considered. Some of these parameters, such as fibrotic layer thickness, hydrogel seeding density, and blood oxygen concentration, were explored in the 1D model above. As the primary purpose of the [redacted] of the [redacted] device is to reduce levels of fibrosis encapsulation, the possibility of a fibrotic layer that does not encapsulate the entire device was modeled in 3D.

Surface plots of oxygen concentration obtained by taking 2D cut planes of the 3D models are shown in Figures 13-17 below. In Figure 13, the surface plot of oxygen concentration for no fibrotic layer is shown.

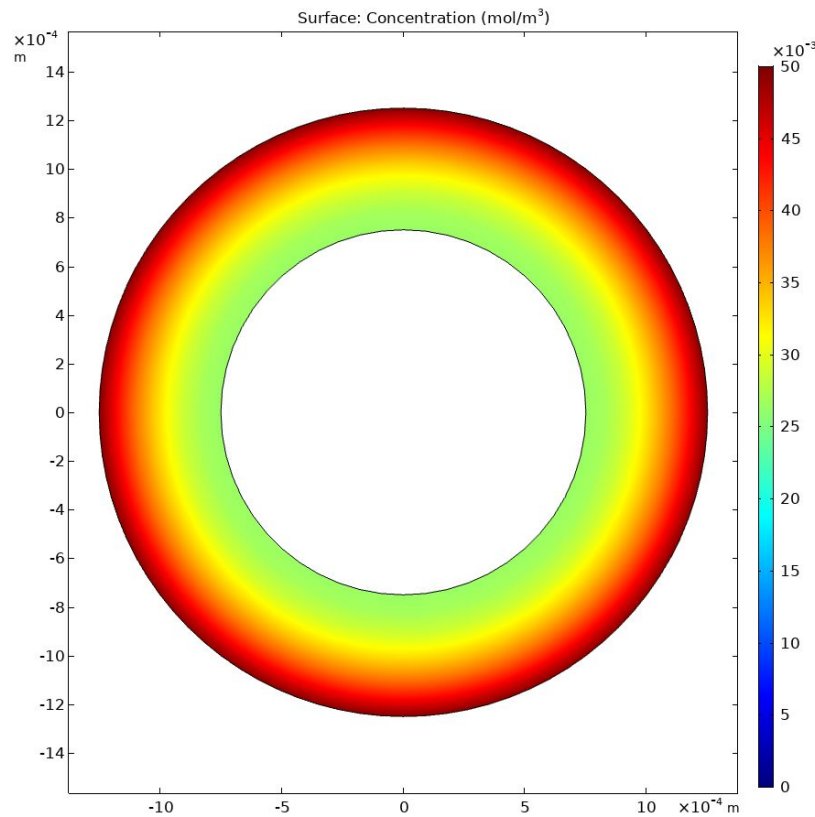


Fig. 13 2D surface plot showing oxygen concentration for a device with no fibrotic layer. Red regions represent the highest oxygen concentrations while green regions represent lower oxygen concentrations at the center of the hydrogel.

Figure 13 shows that the concentration of oxygen remains relatively high throughout the device as seen by the large portions of the plot that are red and orange. These colors represent oxygen concentrations above approximately 0.035 mol/m^3 , which are above the value of 0.033477 mol/m^3 for 50% reduction of insulin production [15]. Even so, there are portions of the device that are yellow and green, which represent values below 0.033 mol/m^3 as seen in the color scale, where insulin production is reduced 50% [15]. This being said, all values of concentration

are well above the critical concentration for cell survival of $1 \times 10^{-4} \text{ mol/m}^3$ [10]. This is expected in a model without fibrosis, although this model is unlikely if not impossible to achieve in vivo. It does, however, show the oxygen concentrations that can be reached and should be the aim, if fibrosis can be significantly reduced.

The model was run for various fibrotic layer thicknesses and percent coverage, as seen in Figures 14-17. First, a $10 \mu\text{m}$ fibrotic layer was studied, with the fibrotic layer covering 25%, 50%, 75% and 100% of the device.

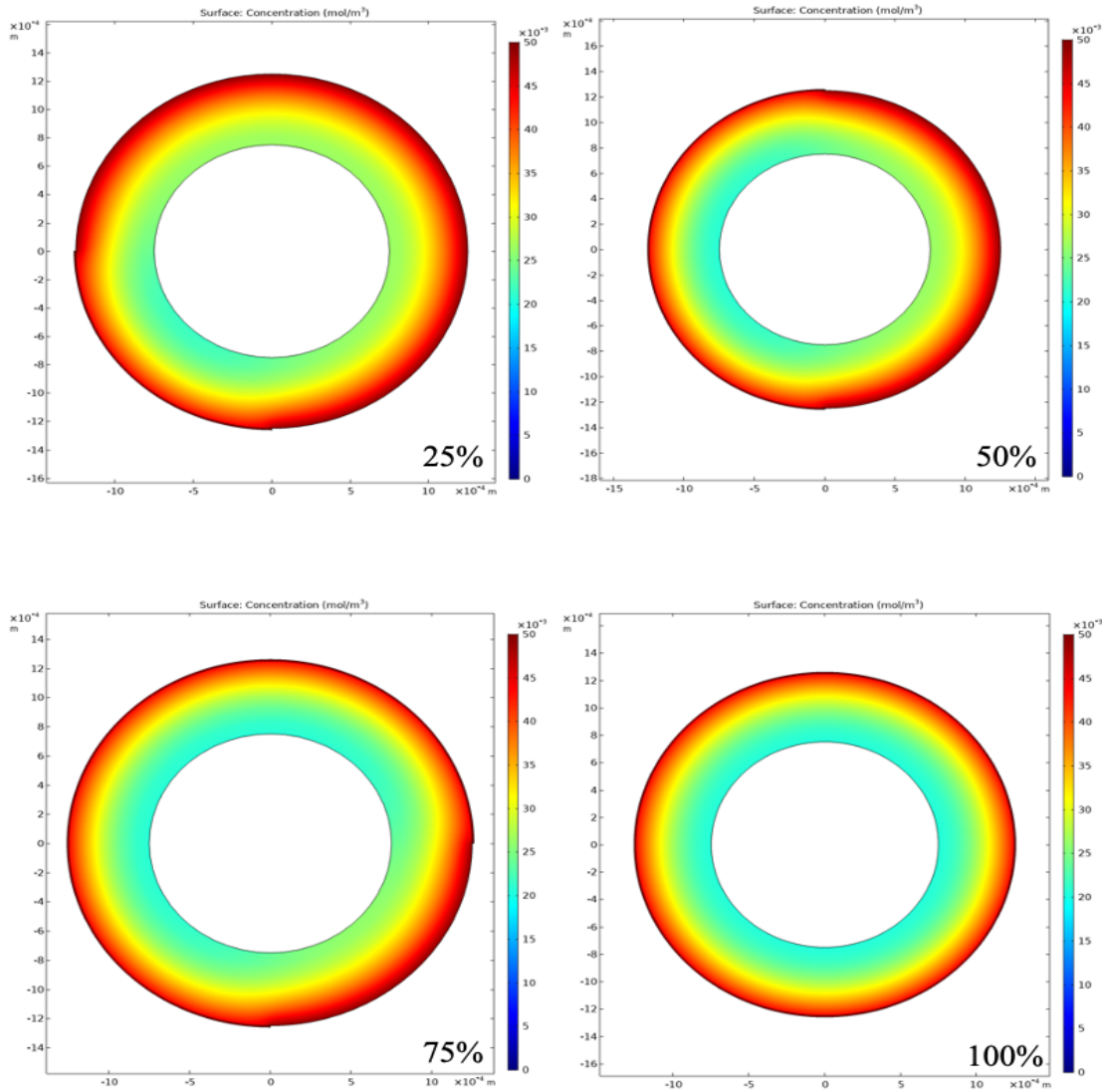


Fig. 14 2D surface plots showing varying levels of fibrosis ranging from 25% to 100% for a $10 \mu\text{m}$ fibrotic layer. The percentage of fibrotic layer coverage can be seen in the bottom right corner of each plot.

When comparing the various percentages of coverage within Figure 14, with 25% on the top left and up to 100% on the bottom right, it is clear that the 10 μ m fibrotic layer has minimal effects on oxygen diffusion. When compared to the model with no fibrotic layer (Figure 13), the similar color scheme shows comparable oxygen levels for all percentages of coverage. That being said, this model still has regions with significantly reduced insulin production, and a larger portion of the device is yellow and green, representing regions where insulin production has decreased over 50% [15]. The device does not approach the critical oxygen concentration for survival of $1 \times 10^{-4} \text{ mol/m}^3$ [10], and instead remains around 0.0225 mol/m^3 , where the green portion of the graph just begins to turn to blue.

The same study as done in Figure 14 was run for a 40 μ m fibrotic layer, and produced dramatically different results, as can be seen in Figure 15.

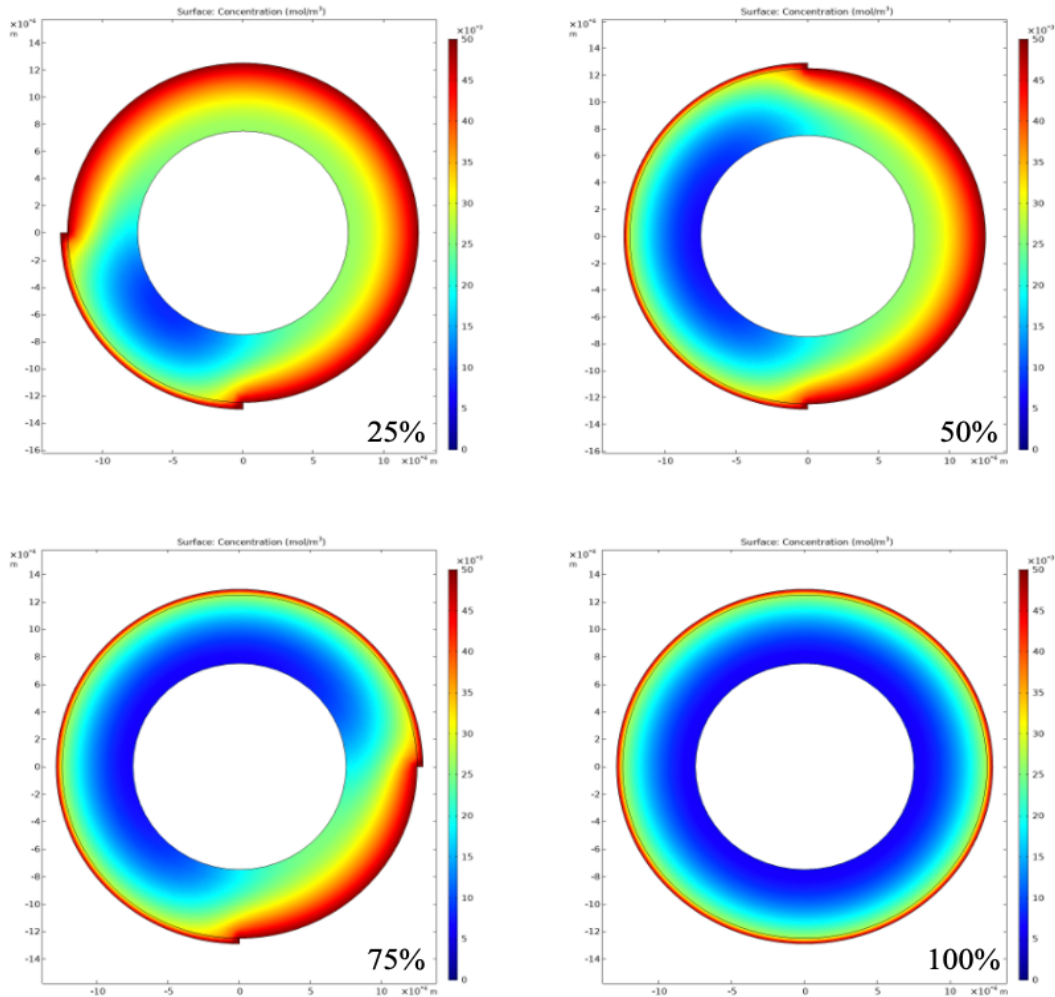


Fig. 15 2D surface plots showing varying levels of fibrosis ranging from 25% to 100% for a 40 μ m fibrotic layer. The percentage of fibrotic layer coverage can be seen in the bottom right corner of each plot. The blue regions represent significantly decreased oxygen concentration.

For a 40 μm fibrotic layer, the change in oxygen concentration in the hydrogel is more noticeable. In Figure 15, the regions of the hydrogel that are significantly affected by fibrotic layer coverage are blue areas near the center. While oxygen concentrations within the hydrogel never reach the critical concentration of $1 \times 10^{-4} \text{ mol/m}^3$, the low concentrations seen in the blue regions encompassing over half the hydrogel device result in a significant reduction of insulin production by cells, approaching, but not yet reaching, the value reported for 98% reduction.

The same study as done in Figure 15 was run for a 100 μm fibrotic layer, resulting in the surface plots seen in Figure 16.

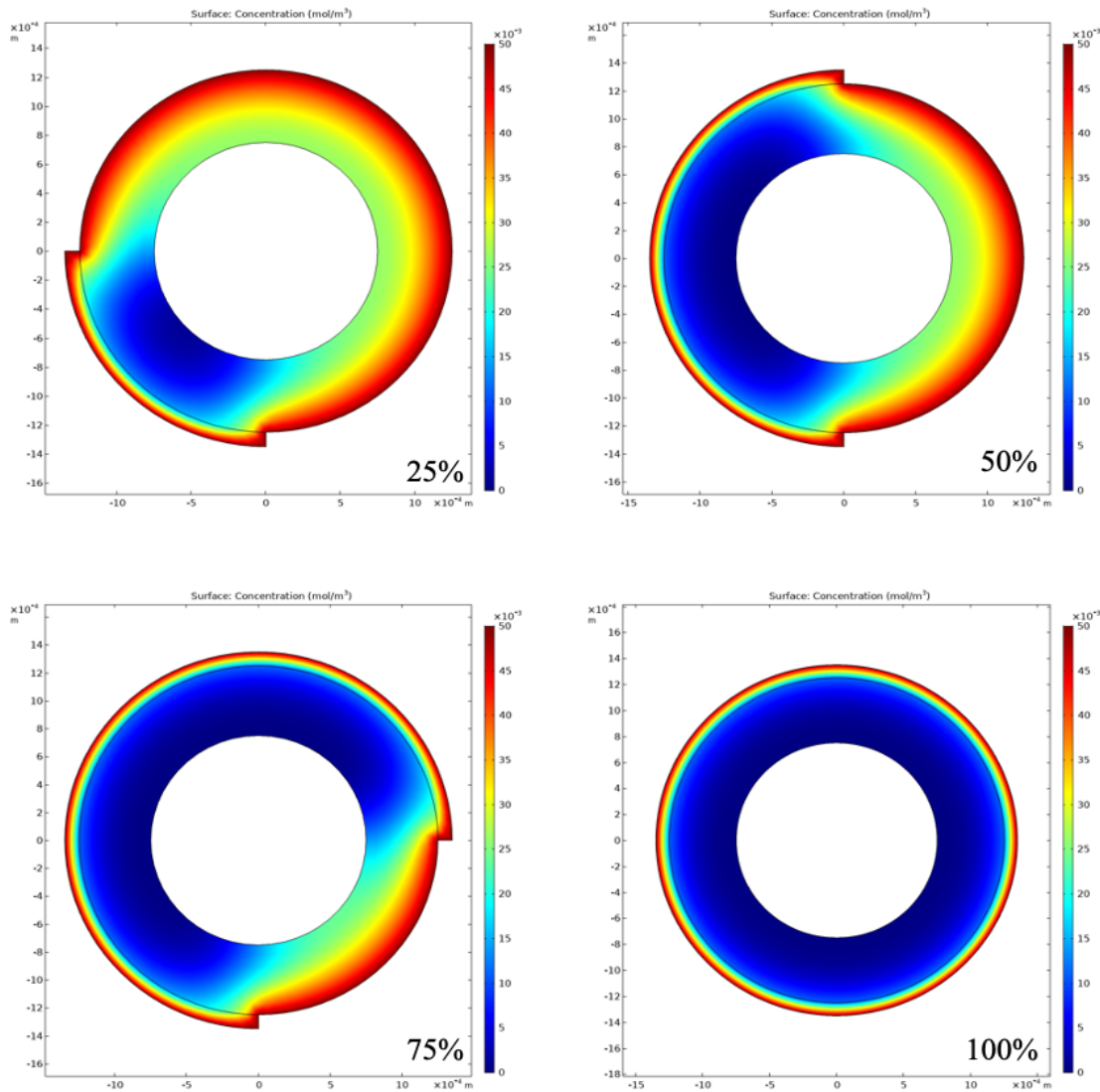



Fig. 16 2D surface plots showing varying levels of fibrosis ranging from 25% to 100% for a 100 μm fibrotic layer. The percentage of fibrotic layer coverage can be seen in the bottom right corner of each plot. Dark blue regions in the hydrogel show severely decreased oxygen concentration.

The 100µm fibrotic layer appears to have drastic effects on the concentration of oxygen in the hydrogel, decreasing it significantly. This can likely be attributed to a combination of diffusive resistance through the fibrotic layer and oxygen-consuming cells within the layer. As seen in Figure 16, the hydrogel regions that have fibrotic layer coverage are entirely dark blue, corresponding to low oxygen concentrations that approach and then reach the critical value of $1 \times 10^{-4} \text{mol/m}^3$. Although the critical value is only found at the dark blue regions near the  core, it is important to note that insulin production and other cellular functions are reduced by up to 50-98% [15] at oxygen levels in the yellow, green, and blue regions, as previously mentioned.

It is clear when looking at progressive plots above that increasing fibrotic layer coverage significantly impedes oxygen concentration. In the plots of 25%, 50%, and 75% coverage, the regions without fibrosis generally have significantly improved oxygen perfusion, with red, orange, yellow and green areas in the hydrogel. When fibrotic layer thickness and coverage increase, the blue regions, where insulin production is almost completely halted and cell death is possible, encompass large portions of the device. The multi-dimensional oxygen transport in this model illustrates the importance of only a slight reduction in the percentage of the device covered in fibrosis: by introducing 2D oxygen transfer, some oxygen is able to reach the hydrogel portion of the device without travelling through the entirety of the fibrotic layer by travelling axially (through the exposed edge of the fibrotic layer) as well as radially.

To show these effects further, the same study was done for a 200µm fibrotic layer, as seen in Figure 17, where fibrosis has detrimental effects on the survivability of encapsulated cells.

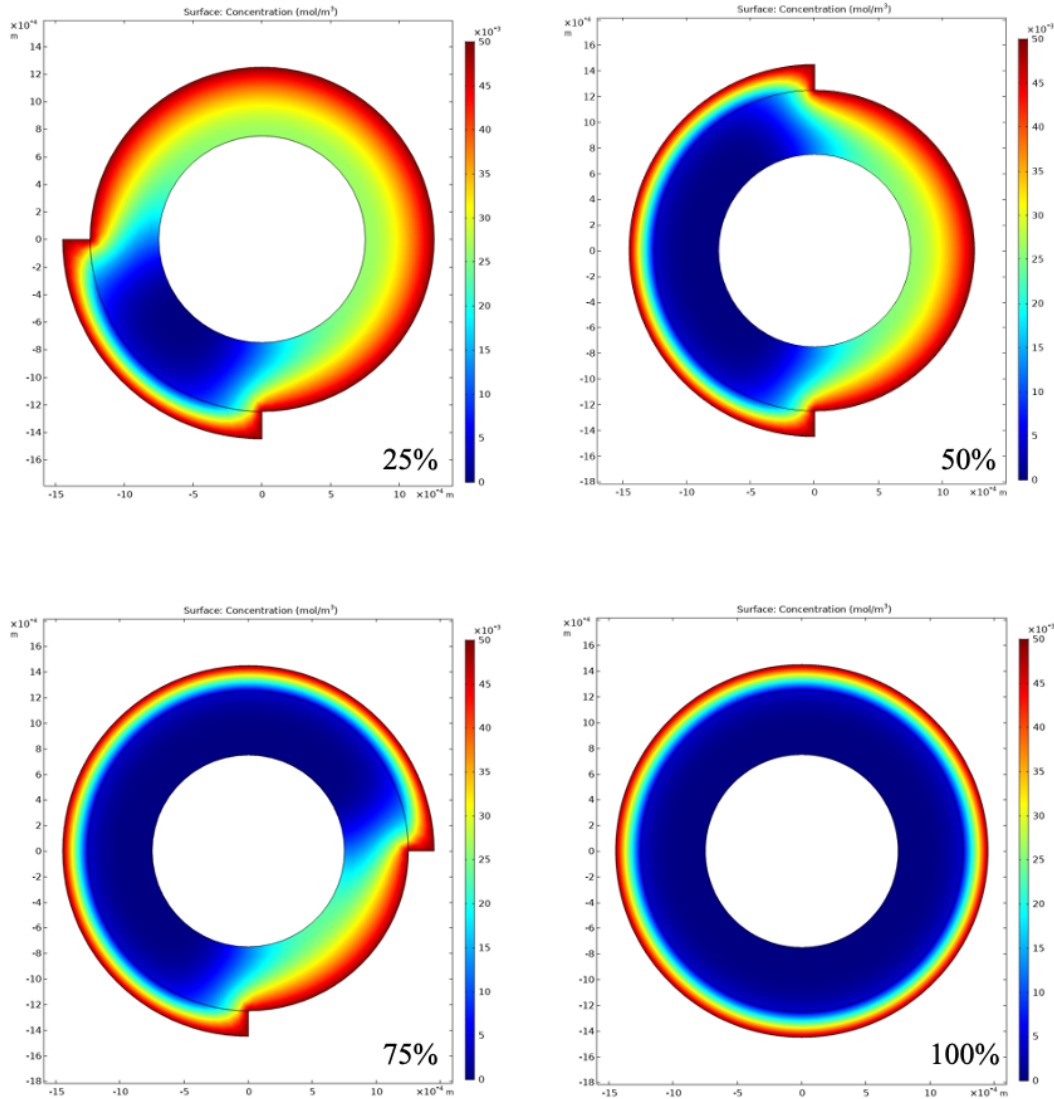


Fig. 17 2D surface plots showing varying levels of fibrosis ranging from 25% to 100% for a $200\mu\text{m}$ fibrotic layer. The percentage of fibrotic layer coverage can be seen in the bottom right corner of each plot. The dark blue areas of the plot show dangerously low oxygen concentrations.

As seen in Figure 17 above, as fibrotic layer coverage increases from 25% on the top left to 100% on the bottom, the dark blue area of the figures significantly increases, while the red, orange, and yellow areas decrease. The dark blue represents dangerously low oxygen concentration, which is indicative of lowered insulin production and cell death. The trend in Figure 17, as was found in Figure 16, is that as the percentage of fibrotic layer coverage increases, the area of the hydrogel with inadequate oxygen perfusion increases. Furthermore, the $200\mu\text{m}$ fibrotic layer is particularly detrimental to cells in the device as it is clear, due to the dark blue coloring, that any percentage of fibrosis coverage results in severe decrease in

oxygen perfusion to the portion of the device that is covered. Only cells in the regions of the device without coverage by the 200 μm fibrotic layer have enough oxygen to survive. Further, only a small portion of these regions are red or orange and able to produce significant amounts of insulin, remaining at oxygen concentrations above 0.033477 mol/m^3 , where insulin production is above 50% [15]. This shows the importance of reducing fibrosis and preventing it from reaching thicknesses as great as 200 μm .

The data from Figures 13-17 were compiled into one graph, which can be seen in Figure 18 below. For each surface plot, the volumetric average oxygen concentration within the hydrogel region was calculated, associating a quantitative value with the trends that were seen in the color schemes above. These values were then plotted based on fibrotic layer thicknesses and percent coverage below.

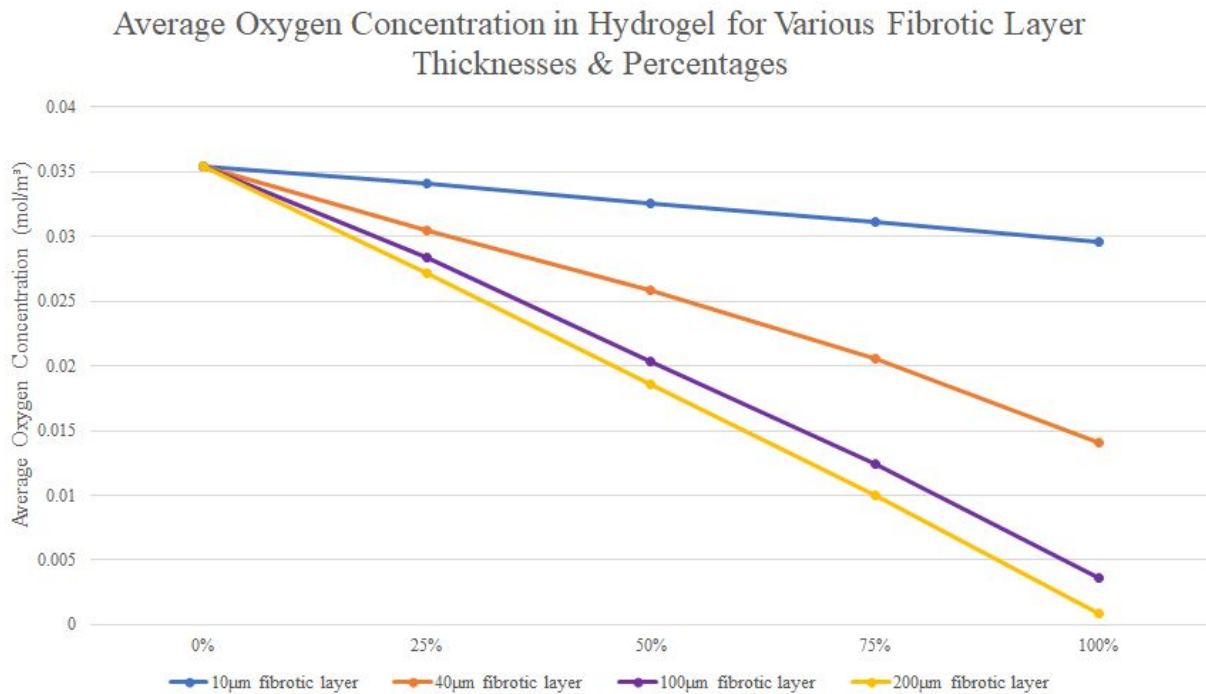


Fig. 18 Line graph showing average oxygen concentration in hydrogel for various fibrotic layer thicknesses and percentages. Calculated using COMSOL volume average function of oxygen concentration in the hydrogel region for each fibrotic layer thickness (10 μm , 40 μm , 100 μm , 200 μm) and each percentage coverage (0%, 25%, 50%, 75%, 100%).

Figure 18 shows the trend that as fibrotic layer thickness and fibrotic layer percent coverage increase, the average oxygen concentration in the hydrogel decreases. Specifically, the slopes of the lines representing the various fibrotic layer thicknesses increase in magnitude with increasing thickness. This shows that the thicker fibrotic layer results in severe oxygen depletion in the device, at the same percentage coverage.

This study of oxygen perfusion is important because the hydrogel contains pancreatic cells, which require adequate oxygen levels to survive and to produce insulin, fulfilling their function of insulin production in the place of functioning pancreatic cells in a patient with diabetes. The functioning of these implanted pancreatic cells depends heavily on oxygen concentration [14]. Therefore, it is evident that decreasing fibrosis as much as possible is an integral part of ensuring that this device functions properly.

5.3 Sensitivity Analysis

A sensitivity analysis was performed to determine how the solution changes as its parameters change, i.e., determining how sensitive the model is to material properties. By adjusting the values of chosen parameters by a certain percentage, in this case ten percent, it is possible to determine the degree of accuracy needed for that input. The sensitivity analysis was performed for the seeding density of cells in the hydrogel layer (ρ_{islets}), the consumption rate of oxygen in the hydrogel ($R_{max, oxy, hydro}$), diffusion of oxygen in the hydrogel ($D_{O_2, hydro}$), the diffusivity of oxygen in the fibrotic layer ($D_{o_2, fib}$), the concentration of oxygen at the surface of the fibrotic layer (C_{tissue}) and the consumption rate of oxygen in the fibrotic layer ($R_{max, oxy, fib}$).

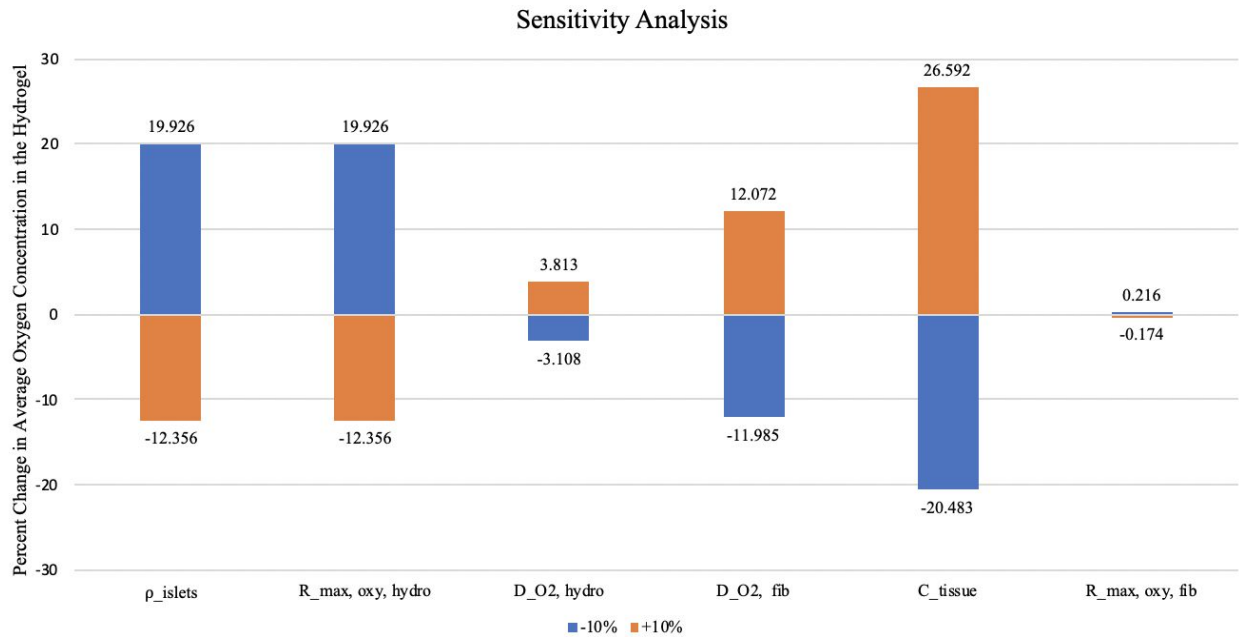



Fig. 19 Sensitivity Analysis of a +/-10% Change in Parameter Values. The model was run using each parameter when increased by 10% and decreased by 10%. Results were used to determine the percent change in the average concentration of oxygen in the hydrogel for each value (baseline, +10%, -10%) and then graphed.

The trend for the diffusivity values of oxygen in the hydrogel and fibrotic layer are the same — as the diffusivity increases, the average concentration of oxygen in the hydrogel increases. This is as expected since increasing the diffusivity, or the ease with which oxygen can travel through the material, would allow oxygen to reach cells located further into the device. However, the sensitivity to the diffusivity values varies between that of the hydrogel and the fibrotic layer. Varying the hydrogel diffusivity by plus/minus 10% led to a significantly smaller change in the average oxygen concentration when compared to varying the diffusivity in the fibrotic layer, implying that the model is less sensitive to this value. Therefore, it can be concluded that the model is more sensitive to the diffusivity of the fibrotic layer.

The sensitivity analysis was also completed for seeding density, surface concentration at the outer model boundary, reaction rate within the hydrogel and reaction rate within the fibrotic layer. As seen in the analysis, three of these variables proved to significantly impact the distance of oxygen diffusion when subjected to the +/-10% change, while the reaction rate in the hydrogel had an insignificant impact. Seeding density and reaction rate in the hydrogel had the same impact on oxygen concentration, as these values are linearly related as seen in Equation 3. There is an inverse relationship between the seeding density and oxygen consumption rate in the hydrogel and the oxygen concentration, and a direct relationship between surface concentration and oxygen concentration. These are as expected: increasing the seeding density/reaction rate increases the number of cells or rate at which they are consuming oxygen, while increasing the surface concentration leads to more oxygen within the device. Finally, changes in the reaction rate within the fibrotic layer were seen to have very minimal effect on the model, which is interesting as it suggests the fibrotic layer can be accurately modeled without knowing difficult-to-measure cell density within the fibrotic layer.

Based on the sensitivity analysis, it is clear that this model is most significantly sensitive to changes in seeding density, reaction rate in the hydrogel, and surface oxygen concentration. The model is also moderately sensitive to changing diffusivity values, with almost no sensitivity to the reaction rate of oxygen within the fibrotic layer. Consequently, it is important to design the model using the most realistic values possible (based on pre-existing literature and the design of the  device) for seeding density within the device, reaction rate within the hydrogel, and oxygen concentration within the tissue, as even small changes in these values will result in drastic changes in the model.

5.4 1D Mesh Convergence

The complete mesh of the 1D model is shown below in Figure 20. In order to minimize discretization error and optimize run time, a parametric sweep of maximum mesh sizes ranging from 0.1 μm to 50 μm was performed. This was done at 1250 μm , a point close to the location where the rate of oxygen diffusion changes at the fibrotic and hydrogel interface. Since the smallest length in the geometry was the fibrotic layer thickness of 40 μm , most of the values for

the parametric sweep were less than $40\mu\text{m}$. The maximum element sizes, mesh elements, degrees of freedom, and oxygen concentrations were obtained from the parametric sweep.

The mesh convergence in Figure 21 below shows that the mesh for the 1D model converges at approximately 511 degrees of freedom or 510 mesh elements. After reaching 510 mesh elements, further refinement of the mesh does not change the concentration of oxygen at this point.

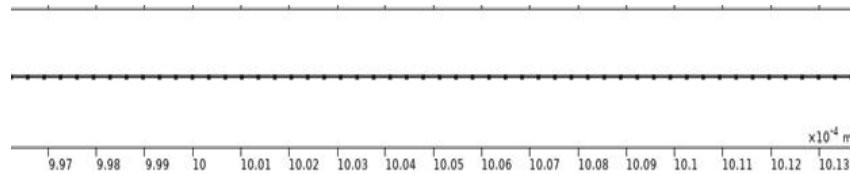


Fig. 20 Mesh plot of the 1D model. The mesh of the 1D model consists of 1492 domain elements.

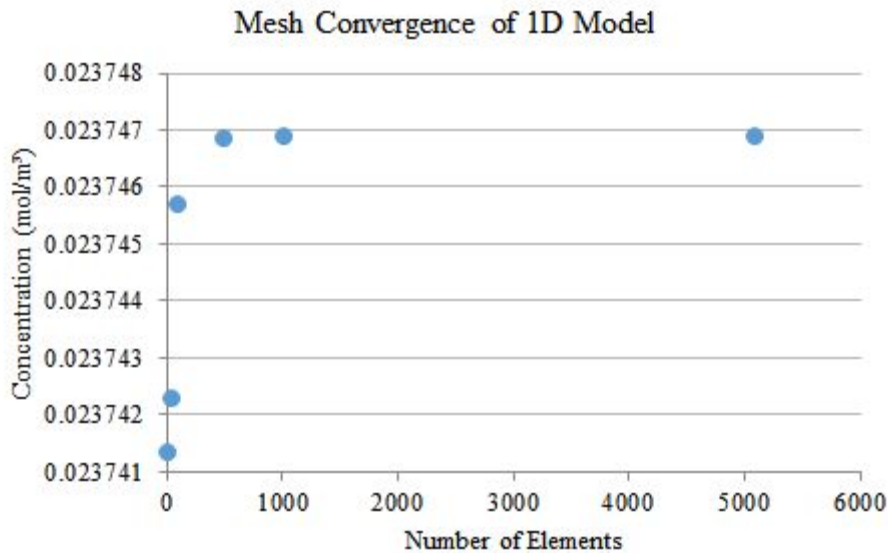


Fig. 21 Mesh convergence plot of the concentration of oxygen vs the degrees of freedom for the 1D model. Based on the graph, the mesh converges at 510 mesh elements. This can be seen as the values for oxygen concentration have no significant change past 510 elements.

5.5 3D Mesh Convergence

The complete 3D mesh is shown below in Figure 22. In order to minimize discretization error and optimize run time, a parametric sweep of maximum mesh sizes was performed. ranging from $60\mu\text{m}$ to $1000\mu\text{m}$ was performed. This was done again at $1250\mu\text{m}$, since this is a point close to the location where the rate of oxygen diffusion changes at the fibrotic and hydrogel

interface. The maximum element sizes, mesh elements, degrees of freedom, and oxygen concentrations were obtained from the parametric sweep.

A mesh convergence was performed near the hydrogel and fibrotic layer interface for the 3D model. Since the smallest length in the 3D geometry was the fibrotic layer thickness of $10\mu\text{m}$, most of the values for the parametric sweep were less than $10\mu\text{m}$. The mesh convergence in Figure 23 below shows that the mesh for the 3D model converges at approximately 1,072,109 mesh elements. Based on these mesh convergences, the number of mesh elements that the 3D model requires is three orders of magnitude higher than the number of mesh elements required by the 1D model. This makes sense given the increase in dimension from 1D to 3D.

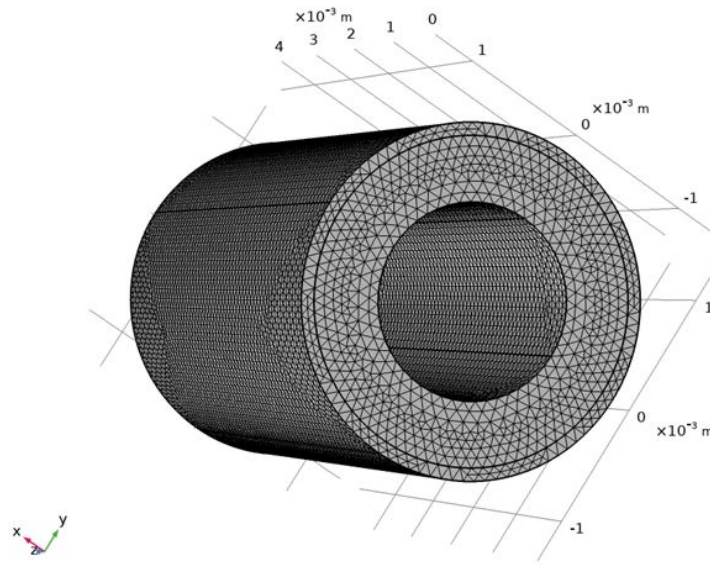


Fig. 22 Mesh plot of the 3D model with $100\mu\text{m}$ fibrotic layer. The mesh of the 3D model consists of 464,350 domain elements.

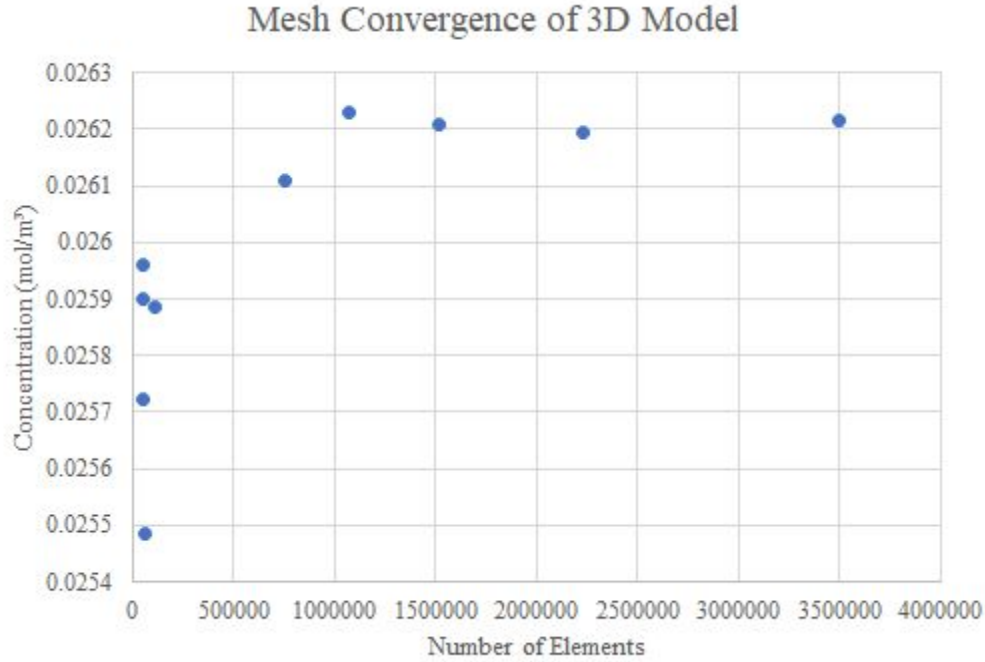


Fig. 23 Mesh convergence plot of the concentration of oxygen vs the degrees of freedom for the 3D model. Based on the graph, the mesh converges at 1,072,109 mesh elements, where the number of elements no longer significantly impacts oxygen concentration.

5.6 Validation

In order to confirm that the model realistically depicts diffusion and reaction, the COMSOL models were compared to other existing models. Currently, there exists no dataset that models gas diffusion through a device with hydrogel components surrounded by a fibrotic layer. Because of this, results from the model were validated by dividing the domain into two separate regions: the fibrotic layer and the hydrogel layer.

Using [8], in which diffusion of oxygen through a fibrotic layer surrounding immunoisolated tissue was measured, oxygen partial pressure was compared over 100 μ m distance for the full fibrotic layer coverage of the device as shown in Figure 24. The slight variations in results between this study's obtained data and that in [8] can be explained by the use of a zero-order approximation instead of the full Michaelis-Menten kinetics adopted in this model and by the possibility of different parameter values as those used in [8] were not available. The zero-order approximation used to implement Michaelis-Menten into an analytical solution in the compared model resulted in a concentration profile more limited by this simplification. Overall, there are clear parallel trends that exist between the concentration profiles, which provide support that the obtained model in this paper matches that of prior conducted research.

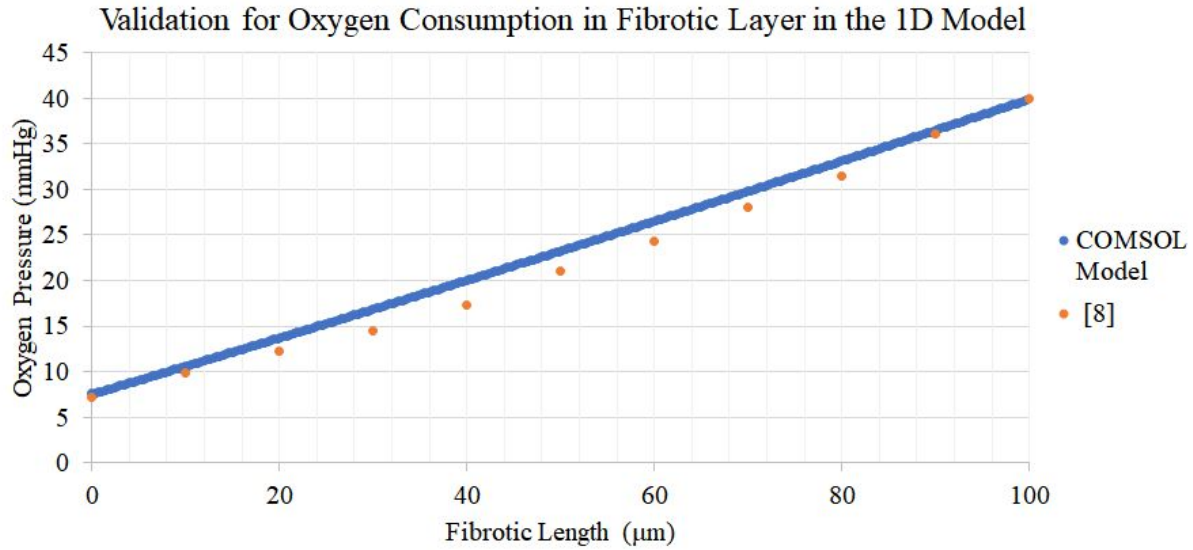


Fig. 24 *Validation for Oxygen Consumption in Fibrotic Layer: 1D Model Compared with 1D Model from Literature.* Graph shows data from the obtained model for oxygen concentration (in mmHg) measured as a function of distance measured from the start of the fibrotic layer. Data obtained from [8], as seen in orange, shows a similar trend in oxygen concentration as in this study, as seen blue.

After comparison of the COMSOL Multiphysics® 1D model with an existing model, it was necessary to do the same with the 3D model and ensure that oxygen concentration measured in the device was comparable to that in an existing biomedical device with a fibrotic layer. Using [16], which explores oxygen concentration through magnetic resonance spectroscopy (MRS), average oxygen partial concentrations were compared between their device and the COMSOL 3D model. As seen in Figure 25, the concentrations are significantly similar. From the original study, the fibrotic length was assumed to have a complete coverage of the device with a thickness of 40μm. These conditions were chosen as they are considered typical for fibrous tissue [17]. Based on support from an existing simplification of an analytical function and from comparing average hydrogel concentrations as a result of a fibrotic layer, there is evidence that the model has a basis in reality for the phenomenon discussed.

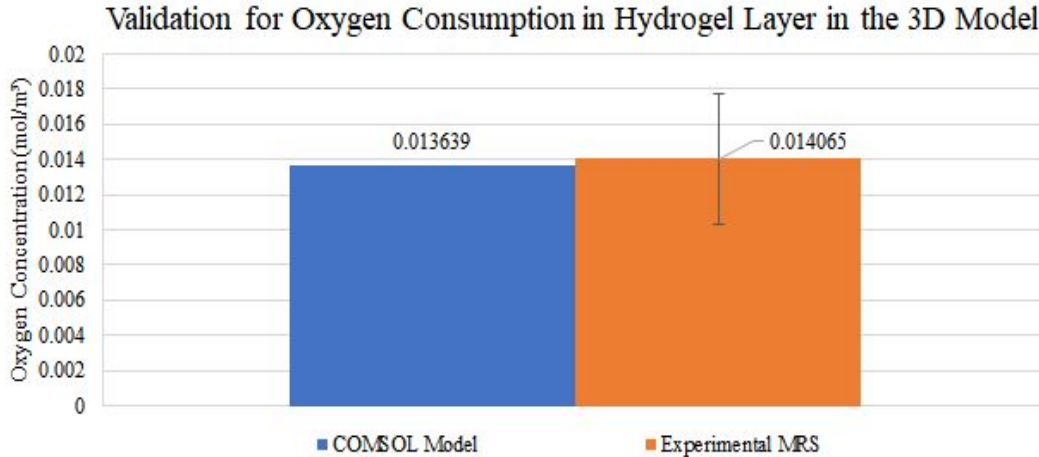


Fig. 25 *Validation for Oxygen Consumption in Hydrogel Layer in the 3D Model.* Graph shows data from the obtained model for oxygen concentration (in mol/m³) in blue. Data obtained from [16] shows a similar value in oxygen concentration, as seen in orange.

6. Conclusion

Results from this study of oxygen transfer within a [redacted] biomedical device with varying fibrosis configurations emphasize the importance of reducing fibrotic layer formation in order to facilitate oxygen transfer to cells within the device. From parametric sweeps conducted in the 1D study, it was found that a thicker fibrotic layer results in less oxygen entering the hydrogel at the hydrogel/fibrotic layer interface. Additionally, it is suggested that for blood concentration levels equivalent to 24mmHg in the body, the device could have limited effectiveness due to the low oxygen concentrations reached near the [redacted] core. It was also concluded that varying macrophage density within the fibrotic layer had a nonsignificant effect on the resulting oxygen concentration profile within the hydrogel.

Through the 3D study, it was learned that while fibrotic tissue encapsulation has very mild effects at 10μm thickness, it becomes a significant problem at 40μm. Further, serious hypoxia is observed at fibrotic tissue thicknesses at 100μm or greater, significantly decreasing the concentration of oxygen throughout the hydrogel. When studying the effects of differing fibrotic layer configurations, it was found that only a slight reduction in the percentage of the device covered in fibrosis has drastic effects on the effectiveness of the [redacted] device: by introducing 2D oxygen transfer, some oxygen is able to reach the hydrogel portion of the device without travelling through the entirety of the fibrotic layer by travelling axially (through the exposed edge of the fibrotic layer) as well as radially. All of these results point to the major conclusion that decreasing fibrosis, either in terms of thickness or in terms of coverage percentage, is an integral part in achieving success for this device.

Finally, based on the sensitivity analysis, it was found that the model is most significantly sensitive to changes in seeding density, reaction rate in the hydrogel, and surface oxygen

concentration. The model is also moderately sensitive to changing diffusivity values, with almost no sensitivity to the reaction rate of oxygen within the fibrotic layer. This should be taken into account when fine tuning the model, as some changes will lead to much more drastic effects than others. This analysis of the device will aid the Ma Laboratory, as many scenarios have been modeled illustrating the effects of different fibrotic tissue coverages on the survival of insulin-producing cells within the device. If these devices are brought to clinical trial, the timeline can be vastly shortened with information about the ideal device dimensions established with this COMSOL Multiphysics® modeling. Future studies building on this existing model could explore the effects of other relevant chemical species, such as insulin and glucose, giving further insight to the possibility of this being an effective method for the treatment of type 1 diabetes.

7. Appendix A: Input Parameters

Table 1. *Geometry Terms*



Parameter	Symbol	Value	Source
Axial Coordinate Direction	z		
Azimuth Direction	φ		
Length (mm)	L	5	See footnote ¹
Radial Direction	r		
Radius of Fibrotic Layer (μm)	r_{fibrotic}	1260 - 1450	See footnote ¹
Radius of Hydrogel Layer (μm)	r_{hydrogel}	1250	See footnote ¹
Radius of  Core (μm)	r_{metal}	750	See footnote ¹
Thickness of Fibrotic Layer (μm)	Fibrotic_Layer	10 - 200	See footnote ¹
Thickness of Hydrogel Layer (μm)	Hydrogel_Layer	500	See footnote ¹
Thickness of  Core (μm)	Metal_Layer	750	See footnote ¹

Table 2. *Michaelis-Menten Kinetics Terms*

Parameter	Symbol	Value	Source
-----------	--------	-------	--------

¹ Confirmed via personal communication with Alexander Ernst

Concentration of Oxygen (mol/m ³)	c_{O_2}		
Critical Concentration of O_2 for Cell Survival (mol/m ³)	$c_{cr, oxy}$	1×10^{-4}	[10]
Concentration of O_2 at $\frac{1}{2} Vmax$ (mol/m ³)	$c_{Hf, oxy}$	0.001	[10]
Rate of O_2 Consumption in the Hydrogel Layer (mol/m ³ · s)	$R_{max, oxy, hydro}$	0.034	[10]
Rate of O_2 Consumption in the Fibrotic Layer (mol/m ³ · s)	$R_{max, oxy, fib}$	2.167×10^{-5} , 1.085×10^{-4} , 2.167×10^{-4} , 1.085×10^{-3}	See footnote ²
Volume Fraction of Cells in Hydrogel Layer	ρ_{islets}	$0.01-0.05$	See footnote ¹

Table 3. Oxygen Transport Terms

Parameter	Symbol	Value	Source
Bunsen Coefficient Solubility of Oxygen in Water (mol · s ² /kg/m ²)	α_{O_2}	9.3×10^{-6}	See footnote ¹
Concentration of O_2 at Fibrotic Outer Layer (mol/m ³)	$c_{surface}$	0.029757 , 0.049596 , 0.074394	[13]
Concentration of O_2 in Tissue Surrounding the Device (mol/m ³)	c_{tissue}	0.050	[10]
Diffusivity of O_2 in Fibrotic Layer (m ² /s)	$D_{O_2, fib}$	4.5×10^{-10}	[11]
Diffusivity of O_2 in Hydrogel Layer (m ² /s)	$D_{O_2, hydro}$	3×10^{-10}	[10]
Pressure of O_2 on Surface of Fibrotic Layer (mmHg)	$P_{surface}$	$24, 40, 60$	[13]
Reaction term for Oxygen (mol/m ³ · s)	R_{oxy}		

¹ Confirmed via personal communication with Alexander Ernst² Calculations shown in Appendix C

8. Appendix B: CPU and Memory Usage

Table 4. *CPU and Memory Usage from Models*

Model	Virtual Memory	Physical Memory	CPU
1D Model	935MB	690MB	7s
Model A, 0% Fibrosis	1489MB	975MB	136s
Model B, 100% Fibrosis	1590MB	852MB	107s
Model C, 25% Fibrosis	1330MB	729MB	266s
Model D, 50% Fibrosis	1455MB	952MB	139s
Model E, 75% Fibrosis	1477MB	622MB	228s

9. Appendix C: Mathematical Methods

9.1 Conversion of Partial Pressure to Concentration of Oxygen

The level of oxygen in the body is normally measured using partial pressure. For the sake of consistency, partial pressure in mmHg was converted to concentration in $\text{mol}/\text{m}^3 \cdot \text{s}$ using the Bunsen coefficient. The relationship between partial pressure and concentration is shown in Equation 11. A sample calculation for a surface partial pressure of 24mmHg is shown below.

$$\begin{aligned}
 c_{O_2} &= \alpha_{O_2} P_{\text{surface}} \\
 c_{O_2} &= (9.3 \times 10^{-6} \frac{\text{mol} \cdot \text{s}^2}{\text{kg} \cdot \text{m}^2}) (24 \text{ mmHg}) (\frac{133.32239 \text{ kg}/\text{m} \cdot \text{s}^2}{1 \text{ mmHg}}) \\
 c_{O_2} &= 0.029757 \frac{\text{mol}}{\text{m}^3}
 \end{aligned} \tag{11}$$

This conversion was used for all partial pressure values used in this paper, including the boundary conditions of 40mmHg and 60mmHg used in the parametric sweep.

9.2 Calculation of Oxygen Consumption Rates in the Fibrotic Layer

Oxygen consumption rate in the fibrotic layer depends on macrophage density in the fibrotic layer. The reaction term for the fibrotic layer was determined from the formula shown in Equation 12, where R_{macro} is the oxygen consumption rate of individual rat macrophages and ρ_{macro} is the macrophage density in the fibrotic layer. A sample calculation for the oxygen consumption rate for a macrophage density of $1 \times 10^6 \text{ cells}/\text{mL}$ is shown below.

$$R_{\text{max, oxy, fib}} = R_{\text{macro}} \rho_{\text{macro}} \tag{12}$$

$$R_{max, oxy, fib} = (2.167 \times 10^{-17} \frac{mol}{cell \cdot s})(1 \times 10^6 \frac{cells}{mL})(\frac{1 mL}{10^{-6} m^3}) = 2.167 \times 10^{-5} \frac{mol}{m^3 \cdot s}$$

This was repeated for macrophage densities of $5 \times 10^6 \frac{cells}{mL}$, $1 \times 10^5 \frac{cells}{mL}$, and $5 \times 10^5 \frac{cells}{mL}$ to obtain the values for $R_{max, oxy, fib}$ in Appendix A.

A value of $130 \frac{pmol}{min \cdot 10^5 cells}$ was selected for R_{macro} from the upper range of oxygen consumption rates measured for rat macrophages [18]. The conversion of this value to $\frac{mol}{cell \cdot s}$ is shown below.

$$(130 \frac{pmol}{min \cdot 10^5 cells})(\frac{1 mol}{10^{12} pmol})(\frac{1 mL}{10^{-6} m^3}) = 2.167 \times 10^{-17} \frac{mol}{cell \cdot s}$$

10. References

- [1] W. Jeffcoate, “Drive to eliminate the burden of type 1 diabetes,” *The Lancet*, vol. 367, no. 9513, pp. 795–797, Mar. 2006, doi: 10.1016/s0140-6736(06)68314-1
- [2] J. A. Noble and A. M. Valdes, “Genetics of the HLA Region in the Prediction of Type 1 Diabetes,” *Current Diabetes Reports*, vol. 11, no. 6, pp. 533–542, Sep. 2011, doi: 10.1007/s11892-011-0223-x
- [3] M. A. Atkinson, G. S. Eisenbarth, and A. W. Michels, “Type 1 diabetes,” *The Lancet*, vol. 383, no. 9911, pp. 69–82, Jan. 2014, doi: 10.1016/s0140-6736(13)60591-7
- [4] J. M. Anderson, A. Rodriguez, and D. T. Chang, “Foreign body reaction to biomaterials,” *Seminars in Immunology*, vol. 20, no. 2, pp. 86–100, Apr. 2008, doi: 10.1016/j.smim.2007.11.004
- [5] N. N. Le, M. B. Rose, H. Levinson, and B. Klitzman, “Implant Healing in Experimental Animal Models of Diabetes,” *Journal of Diabetes Science and Technology*, vol. 5, no. 3, pp. 605–618, May. 2011, doi: 10.1177/193229681100500315
- [6] D. An, et al., “Designing a Retrievable and Scalable Cell Encapsulation Device for Potential Treatment of Type 1 Diabetes,” *PNAS*, vol. 115, no. 2, pp. E263-272, Dec. 2017, doi: 10.1073/pnas.1708806115
- [7] A. U. Ernst, L.-H. Wang, and M. Ma, “Islet encapsulation,” *Journal of Materials Chemistry B*, vol. 6, no. 42, pp. 6705–6722, Sep. 2018, doi: 10.1039/c8tb02020e
- [8] E. S. Avgoustiniatos and C. K. Colton, “Effect of External Oxygen Mass Transfer Resistances on Viability of Immunoisolated Tissues,” *Annals of the New York Academy of Sciences*, vol. 831, no. 1, pp. 145–166, Dec. 2006, doi: 10.1111/j.1749-6632.1997.tb52192.x
- [9] R. Cao, E. Avgoustiniatos, K. Papas, P. Vos, and J. R. T. Lakey, “Mathematical predictions of oxygen availability in micro- and macro-encapsulated human and porcine pancreatic islets,” *Journal of Biomedical Materials Research Part B: Applied Biomaterials*, vol. 108, no. 2, pp. 343–352, Apr. 2019, doi: 10.1177/0196859917735650
- [10] P. A. Buchwald, “A local glucose-and oxygen concentration-based insulin secretion model for pancreatic islets,” *Theoretical Biology and Medicine Modelling*, vol. 8, no. 1, pp. 1-25, Jun. 2011, doi: 10.1186/1742-4682-8-20
- [11] U. Cheema, Z. Rong, O. Kirresh, A. J. MacRobert, P. Vadgama, and R. A. Brown, “Oxygen diffusion through collagen scaffolds at defined densities: implications for cell survival in tissue models,” *Journal of Tissue Engineering and Regenerative Medicine*, vol. 6, no. 1, pp. 77–84, Oct. 2011, doi: 10.1002/term.402
- [12] A. S. Lewis, “Eliminating oxygen supply limitations for transplanted microencapsulated islets in the treatment of type 1 diabetes,” Ph.D dissertation, Dept. of Chemical Engineering, MIT., Cambridge, MA, 2008. Accessed on: April 22, 2020. [Online]. Available: <http://hdl.handle.net/1721.1/42941>

- [13] M. A. Bochenek, et al., “Alginate encapsulation as long-term immune protection of allogeneic pancreatic islet cells transplanted into the omental bursa of macaques,” *Nature Biomedical Engineering*, vol. 2, no. 11, pp. 810–821, Aug. 2018., doi: 10.1038/s41551-018-0275-1
- [14] T. T. Braga, J. S. H. Agudelo, and N. O. S. Camara, “Macrophages During the Fibrotic Process: M2 as Friend and Foe,” *Frontiers in Immunology*, vol. 6, Nov. 2015, doi: 10.3389/fimmu.2015.00602
- [15] K. E. Dionne, C. K. Colton, and M. L. Yarmush, “Effect of hypoxia on insulin secretion by isolated rat and canine islets of Langerhans,” *Diabetes*, vol. 42, no. 1, pp. 12–21, Jan. 1993. doi: 10.2337/diabetes.42.1.12
- [16] S. A. Einstein, B. P. Weegman, M. T. Firpo, K. K. Papas, and M. Garwood, “Development and Validation of Noninvasive Magnetic Resonance Relaxometry for the In Vivo Assessment of Tissue-Engineered Graft Oxygenation,” *Tissue Engineering Part C: Methods*, vol. 22, no. 11, pp. 1009–1017, Nov. 2016, doi: 10.1089/ten.tec.2016.0106
- [17] D. Akilbekova and K. M. Bratlie. “Quantitative Characterization of Collagen in the Fibrotic Capsule Surrounding Implanted Polymeric Microparticles through Second Harmonic Generation Imaging,” *PLOS ONE*, vol. 10, no. 6, pp. 1-17, Jun. 2015, doi: 10.1371/journal.pone.0130386
- [18] V. Serbuleaa, et al. “Macrophage phenotype and bioenergetics are controlled by oxidized phospholipids identified in lean and obese adipose tissue,” *PNAS*, vol.115, no. 27, pp. E6254–E6263, Jun. 2018, doi: 10.1073/pnas.1800544115